

The translation initiation factor eIF3M2 upregulates HEAT SHOCK PROTEIN 70 to maintain pollen tube membrane integrity during heat shock

Zahra Kahrizi,^{1,2,†} Christos Michailidis,^{1,†} Karel Raabe,^{1,2} Vinod Kumar,^{1,2} David Honys,¹ Said Hafidh^{1,*}

¹Laboratory of Pollen Biology, Institute of Experimental Botany of the Czech Academy of Sciences, Rozvojová 263, 165 00 Prague 6, Czech Republic

²Department of Experimental Plant Biology, Faculty of Science, Charles University, Viničná 5, 128 44 Praha 2, Czech Republic

*Author for correspondence: hafidh@ueb.cas.cz

[†]First coauthor

The author responsible for distribution of materials integral to the findings presented in this article in accordance with the policy described in the Instructions for Authors (<https://academic.oup.com/plphys/pages/General-Instructions>) is: Said Hafidh (hafidh@ueb.cas.cz).

Abstract

Pollen germination and pollen tube (PT) growth are extremely sensitive to high temperatures. During heat stress (HS), global translation shuts down and favors the maintenance of the essential cellular proteome for cell viability and protection against protein misfolding. Here, we demonstrate that under normal conditions, the Arabidopsis (*Arabidopsis thaliana*) eukaryotic translation initiation factor subunit *eif3m1/eif3m2* double mutant exhibits poor pollen germination, loss of PT integrity and an increased rate of aborted seeds. Surprisingly, under HS at 37 °C, *eif3m1* pollen germination outperformed wild-type Col-0, showing enhanced PT integrity. We established that the improved thermotolerance of the *eif3m1* PT was due to increased expression of its putative paralog eIF3M2, which in turn upregulated Heat Shock protein 70 (HSP70) mRNA and protein levels. Indeed, eIF3M2 overexpression upregulated HSP70 expression, whereas *eif3m2* knockdown showed reduced HSP70.1 promoter activity and increased in PT burst under HS conditions. Moreover, we show that eIF3M2 coimmunoprecipitates with HSP70 in PTs and directly interacts with cytoplasmic HSP70.1/2/4 and eIF4G in *Nicotiana benthamiana* pavement cells. Collectively, our data revealed that plants employ the eIF3M2-HSP70 module as a regulator of thermotolerance to maintain PT membrane integrity and improve fertilization and seed set adaptation under high temperatures.

Introduction

In angiosperms, a robust pollen tube (PT) growth transports a pair of nonmotile sperm cells through the female pistil tissues to maintain efficient fertilization (Hafidh et al. 2016; Johnson et al. 2019). Once PT reaches the female gametophyte, it bursts and releases the 2 sperm cells to fertilize the egg cell and the central cell in the so-called double fertilization event (Hater et al. 2020; Hafidh and Honys. 2021). To fuel this fast journey down the pistil, mature pollen stores high amounts of reserves, including protein coding mRNAs, which are later utilized in an extensive translation to facilitate the growth of the extending PTs (Honys et al. 2009; Hafidh et al. 2018). This was extensively studied in the analysis of tobacco (*Nicotiana tabacum*) PTs, which revealed that monosome-associated ribonucleoprotein particles (EPP granules) facilitate storage of translationally silent mRNAs in mature pollen grains that are later translated in mass upon pollen hydration and during PT growth (Hafidh et al. 2018; Billey et al. 2021; Sze et al. 2021).

All eukaryotes share the same underlying translational mechanisms, which are mostly controlled at the initiation stage of translation by the translation initiation factors (eIFs). These initiation factors are involved in a variety of activities throughout the vegetative and reproductive growth, including embryogenesis and pollen germination (Dutt et al. 2015; Raabe et al. 2019). Plants have evolved translational control specifically based on their requirements, allowing control of expression of a wide

variety of regulators, stress factors, and other proteins in response to distinct stress responses. These significant shifts in translation rates rapidly occur in HS response and hydration of seed or pollen (Browning and Bailey-Serres 2015; Urquidi Camacho et al. 2020). Several studies have demonstrated improved plant resistance to various stresses through modulation of protein translation regulation (Son et al. 2023). However, very little is known about the mechanisms of translational control in response to environmental stresses.

Heat stress in reproductive tissues poses a substantial threat to plant fertilization success, particularly affecting pollen development and PT integrity (Kotak et al. 2007; Hedhly et al. 2009; Chaturvedi et al. 2021). In the process of acclimation, plants developed complex molecular responses against heat stress. Under heat shock (HS) conditions, global gene expression and translation typically shuts down to conserve resources and restricts to produce only essential proteins that protect against cellular damage (Kotak et al. 2007; Dai and Zhu 2020). Specialized proteins such as heat shock protein (HSP) production contribute to plant heat shock response (HSR) (Ohama et al. 2016). The accumulation of HSPs under the control of heat shock transcription factors (HSFs) has been reported to play a key role in the HSR and acquired thermotolerance in plants (Chaturvedi et al. 2021; Berka et al. 2022). HSPs function by acting as molecular chaperones protecting proteins from the negative effects of HS (e.g. conformation changes and protein aggregation), thereby maintaining protein

Received July 26, 2024. Accepted October 9, 2024.

© The Author(s) 2025. Published by Oxford University Press on behalf of American Society of Plant Biologists. All rights reserved. For commercial re-use, please contact reprints@oup.com for reprints and translation rights for reprints. All other permissions can be obtained through our RightsLink service via the Permissions link on the article page on our site—for further information please contact journals.permissions@oup.com.

homeostasis and cell viability during stress (Chaturvedi et al. 2021; Berka et al. 2022). Arabidopsis contains over 200 HSPs belonging to 6 different families, namely Hsp20, Hsp40, Hsp60, Hsp70, Hsp90, and Hsp100 (Tiwari et al. 2021). Along with their chaperone functions, HSPs assist in plant development processes and response to abiotic and biotic stress conditions (Park and Seo 2015; Usman et al. 2017; Ul Haq et al. 2019).

The Arabidopsis HSP70 gene family consists of 18 members with HSP70.1, HSP70.2, HSP70.3, HSP70.4, and HSP70.5 localizing in cytoplasm (Lin et al. 2001). HSP70s are involved in stress-related processes, including the prevention of protein aggregation and solubilization of aggregated proteins, and facilitate refolding of misfolded or unfolded proteins (Rosenzweig et al. 2019). Downregulation of HSP70s has been reported in Arabidopsis to increase thermal sensitivity and developmental defects in Arabidopsis (Sable et al. 2018). HSP70s are also the most upregulated genes among the HSP members under stress conditions inferring their central role in HSR (Matsuoka et al. 2019). For instance, HSP70.3 and HSP70.4 exhibited a considerable transcriptional increase in sperm cells after HS application (Li et al. 2016). HSP70 significantly improved the viability of cryopreserved *Paeonia lactiflora* pollen by enhancing antioxidant enzyme activity, reducing reactive oxygen species (ROS) and malondialdehyde levels, and modulating Ca²⁺ signaling to inhibit apoptosis-like programmed cell death events (Ren et al. 2019). HSP70 in tobacco PTs binds to microtubules in an ATP-dependent manner to maintain PT integrity facilitated by the presence of the 90-kDa kinesin (Parrotta et al. 2013). The 90-kDa kinesin promotes the binding (but not the release) of HSP70 to microtubules, suggesting a cooperative mechanism between these proteins in maintaining the cytoskeleton structure and therefore cell integrity (Parrotta et al. 2013).

Variations in the concentration of HSP70 can influence the interaction between HSP70 and Hsf1, resulting in the displacement of Hsf1 from DNA and the control of HS gene transcription levels (Kmieciak et al. 2020). Mathematical modeling and live cell imaging techniques have demonstrated the dynamics of HSP70 nuclear localization in response to stress and demonstrated how different subsets of the HSR regulon converged to function as auxiliary feedback mechanisms controlling HSP70 subcellular localization under varying conditions (Garde et al. 2024).

The majority of studies on translation regulation in eukaryotes have been performed in yeast and mammals (Tahmasebi et al. 2019; Llácer et al. 2021), where eukaryotic translation initiation factor 3 (eIF3) plays a crucial and multifaceted role (Valášek et al. 2017). eIF3 is the largest complex of all the eIFs, comprising 12 subunits. However, not all eIF3 subunits are essential for protein synthesis, cell growth, and survival (Wagner et al. 2016). eIF3 plays a role in canonical assembly of the preinitiation complex and start codon scanning, but it is also important the regulation of translation at both global and specific levels (Valášek et al. 2017). For example, it has been reported that in yeast, eIF3d and eIF3e comprise a module that specifically stimulates the synthesis of membrane-associated proteins, such as subunits of the mitochondrial electron transport chain (ETC) (Sha et al. 2009). Similarly, eIF3f interacts with proteins that bind Mouse PIWI-like protein 1 (MIWI) piRNAs in 3'-UTRs to circularize mRNA, which promotes sperm-specific translation in mouse (Dai et al. 2019), while eIF3g was recently linked to neuron-specific translation in *Caenorhabditis elegans* by preferential binding of eIF3g to 5'-UTRs (Blazie et al. 2021). Furthermore, in mice, eIF3c is not essential for global translation or viability but directs the translation of the Sonic Hedgehog receptor PTCH1 via a

pyrimidine-rich motif in the 5'-UTR (Fujii et al. 2021). In *C. elegans*, the eIF3k/l module is not required for survival and its depletion increases stress tolerance, likely through mRNA-selective translation modifications (Cattie et al. 2016; Shah et al. 2016; Dai and Zhu 2020; Lin et al. 2020; Duan et al. 2023). In addition, Cap-independent initiation mediated by eIF3 is advantageous in stress conditions by increasing eIF2 binding to HSP70 mRNA where cap-dependent initiation is hindered (Wolf et al. 2020).

In plants, the eIF3 architecture closely resembles the structure of mammalian eIF3 complex comprising 12 subunits (A to M, without J subunit) in Arabidopsis and rice (reviewed in Raabe et al. 2019). Arabidopsis contains 19 coding sequences for the eIF3 complex subunits in its genome with 5 eIF3 subunits encoded by a single gene (eIF3A, eIF3E, eIF3F, eIF3H, and eIF3K) and 7 of the subunits being encoded by 2 genes (eIF3B, eIF3C, eIF3D, eIF3G, eIF3I, eIF3L, and eIF3M) (Browning and Bailey-Serres 2015). Studies of specific plant eIF3 subunits have shown a number of regulatory roles outside their core function in translation initiation.

eIF3M is the last identified subunit in the complex, which is conserved from fission yeast to higher eukaryotes. eIF3M is crucial to the preservation of the structural integrity of the eIF3 complex (Zeng et al. 2013). eIF3M stabilizes 2 of the eIF3 subunits, eIF3F and eIF3H, via subcomplex formation. As a result, eIF3M is needed for eIF3 structural stability and translation initiation function (Zeng et al. 2013; Wagner et al. 2016). eIF3M is required for embryonic development and liver homeostasis in mature mice (Zeng et al. 2013); however, the function of eIF3M in plants is currently unknown. In Arabidopsis, 2 genes code for eIF3M: *AtEIF3M1* (At3g02200) and *AtEIF3M2* (At5g15610) that share 76% sequence identity at the protein level. Both genes are expressed in 2 splicing isoforms. Previous analysis of the *eif3m1* allele did not reveal developmental defects and double mutant *eif3m1 eif3m2* showed no detectable phenotypic differences to wild type (Roy et al. 2011).

In this study, we characterized eIF3M-mediated regulation of translation during male gametophyte development in Arabidopsis. We show that *AtEIF3M1* and *AtEIF3M2* translational fusions were expressed during the male gametophyte development and localized in the nucleus and the cytoplasm of the vegetative cell in pollen. Loss-of-function alleles of eIF3M1 and eIF3M2 T-DNA insertions, *eif3m1* and *eif3m2*, revealed defect in pollen development and in vitro pollen germination and significantly impacted PT growth. Under HS conditions at 37 °C, we established a link between eIF3M2 and HSP70 expression at both transcript and protein levels, leading to an improved PT integrity and PT growth at high temperature. We further showed that eIF3M2 alone coimmunoprecipitate and directly interacts with HSP70 paralogs. Our study revealed that eIF3M is important for male gametophyte development and that eIF3M2 solely promotes HS thermotolerance in PTs by upregulating HSP70 expression levels and reduces production of ROS.

Results

eif3m2 mutant exhibits reduced levels of HSP70 during

To understand the gametophytic role of eIF3M under normal and HS conditions, we generated homozygous T-DNA insertion alleles of *eif3m1* and *eif3m2* and investigated eIF3M function in the gametophyte (Supplementary Fig. S1, A and B). No convincing sporophytic phenotypes were observed under normal conditions. The male germ unit (MGU) consists of a closely associated vegetative nucleus and sperm cell pair formed during pollen formation

(Lalanne and Twell 2002). When we stained pollen nuclei of Col-0, we observed <5% ($n = 354$) aberrant pollen with defects in the positioning of the MGU, whereas *eif3m1-1* and *eif3m1-2* homozygous lines showed 14.8% ($n = 302$) and 17.4% ($n = 289$) aberrant pollen, respectively (Supplementary Fig. S1, C, D, and I). When combined (*eif3m1-1* and *eif3m2-1*), *eif3m1eif3m2* double homozygous lines showed an increase to 31.9% ($n = 338$) of the pollen MGU defect in the form of smaller pollen grains and displaced MGU positioning (Supplementary Fig. S1, C, D, and I).

We next analyzed pollen germination defects in vitro. In Col-0, 75.1% ($n = 365$) of wild-type pollen grains germinated. In contrast, only 26.2% of *eif3m1-1* ($n = 382$) and 22.9% of *eif3m1-2* ($n = 402$), and 33.28% of *eif3m2-1* ($n = 405$) and 30.7% of *eif3m2-2* ($n = 361$) germinated to produce a defined PT (Supplementary Fig. S1, G, H, and K). In *eif3m1* and *eif3m2*, a population of pollen grains initially germinated but then immediately burst and therefore were not considered as germinated PTs (Supplementary Fig. S1, G, H, and K). Of note, the in vitro germination and PT growth phenotype of *eif3m1* and *eif3m2* were not observed when we analyzed their growth in wild-type pistils, suggesting that a sporophytic support of the PT growth through the style is maintained between the wild type and *eif3m1* and *eif3m2* mutants (Supplementary Fig. S2, A to E). The seed abortion was only observed in *eif3m1-2* (20.8%) and *eif3m1/eif3m2* double mutant (27.1%), but not in *eif3m2* single mutants (Supplementary Fig. S1, E, F, and J).

To test whether eIF3M could play a role in HSR, we performed HS experiments to determine how HS affects pollen germination

in *eif3m1* and *eif3m2* mutant lines. Under the HS condition at 37 °C, there was a decreased ratio of pollen germination in wild-type Col-0 and in *eif3m2* single mutant but not in *eif3m1* single mutant (Fig. 1A). Instead, *eif3m1* exhibited an increase in the ratio of germinated pollen (Fig. 1, A and B). Intriguingly, we identified that when the *eif3m1-1* and *eif3m1-2* mutants were subjected to HS, transcripts encoding HSP70 and the HSP70 protein levels were elevated in PTs (Fig. 1, C to E). In contrast, *eif3m2-1* and *eif3m2-2* mutants, when subjected to HS, showed a significant reduction in HSP70 expression compared to *eif3m1* mutants under heat stress conditions (Fig. 1, C to E). Simultaneously, we identified that in the *eif3m1-1* and *eif3m1-2* single mutants, the expression levels of eIF3M2 were also highly upregulated particularly under HS conditions (Fig. 1D). These results provide a possible link between eIFM2 and HSP70 expression dynamics during HSR and a likely crosstalk regulation between eIF3M1 and eIF3M2 that position eIFM2 upstream of HSP70-mediated HSR.

eIFM2 and HSP70 native promoter activities increase during HS

To verify and investigate the link we observed between eIF3M2 and HSP70 expression dynamics under HS condition, we cloned 1,000 bp promoter fragments upstream of the translation start codon of eIF3M1, eIF3M2, and HSP70.1 genes and fused them to GFP-GUS reporter. We then selected single insertion stable Arabidopsis lines of pEIF3M1::GFP:GUS, pEIF3M2::GFP:GUS, and pHSP70::GUS:YFP to

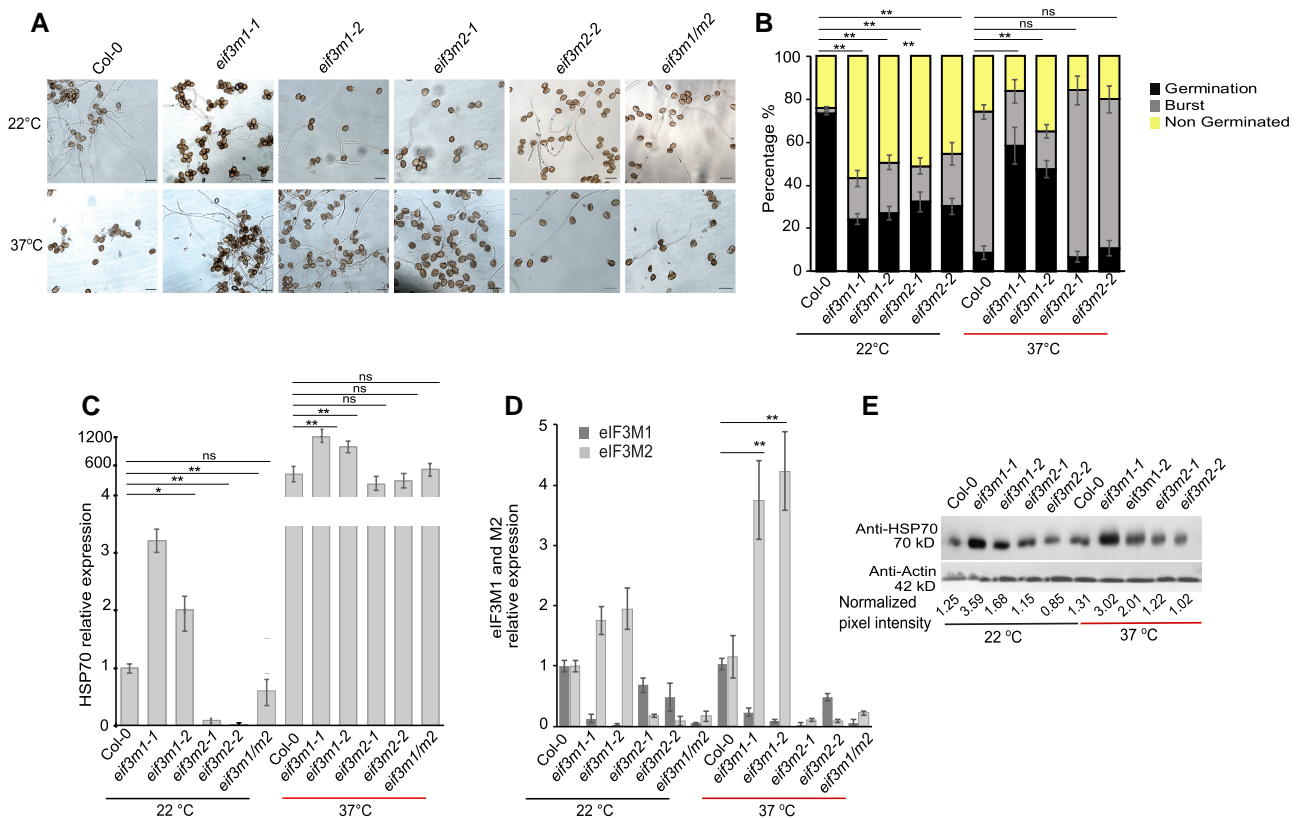


Figure 1. *Eif3m2* mutant is heat sensitive and shows reduced levels of HSP70 expression. **A)** In vitro PT growth of wild-type Col-0, 2 alleles of *eif3m1* and *eif3m2* mutants, and *eif3m1/eif3m2* double mutant under the control and HS conditions. Scale bar: 50 μ m. **B)** Comparison of germination efficiency and PT burst frequency under normal and HS conditions. **C, D)** qPCR analysis of HSP70, eIF3M1, and eIF3M2 levels in PTs of Col-0, *eif3m1*, *eif3m2*, and *eif3m1/m2* double mutants. **E)** Western blot detection of HSP70 protein levels using native HSP70 antibody in *eif3m1* and *eif3m2* mutant PTs under the control and HS conditions. Pixel intensities were measured using ImageJ plugin and normalized to corresponding actin band. Graph data are means (\pm SD). Statistical differences compared with the Col-0 samples were determined using Student's t tests: ** $P < 0.01$, * $P < 0.05$, ns: not significant difference. Same statistical approach was applied to all comparisons shown in this figure.

perform GUS expression analysis. GUS staining was performed on 8-d-old seedlings and flowers grown under 3 different conditions: control temperature at 22 °C, HS at 37 °C, or 45 °C for 1 h followed by a recovery period of 24 h at 22 °C after the HS (Fig. 2, A to D). No GUS staining was observed with *eIF3M1*, *eIF3M2*, or *HSP70* at 22 °C, suggesting no or negligible promoter activities under normal control condition (Fig. 2, A to D). When subjected to HS, an increase in promoter activity was observed for *eIF3M2* and *HSP70.1* promoters but not for *eIF3M1* in whole flowers, mature pollen grains,

and 8-d-old seedlings (Fig. 2, A, B, and D). Following a 24-h recovery period, both *eIF3M2* and *HSP70* exhibited increased levels of promoter activities in all tissues analyzed (Fig. 2, A, B, and D). In support, qPCR and western blot analysis revealed a significant increase in GFP protein accumulation in the promoter lines of *eIF3M2* and *HSP70* genes under the HS and following recovery, compared to expression under control conditions (Supplementary Fig. S3, A and B). Our findings on promoter-reporter analysis support that *eIF3M2* and *HSP70.1* promoters are strongly activated upon HS.

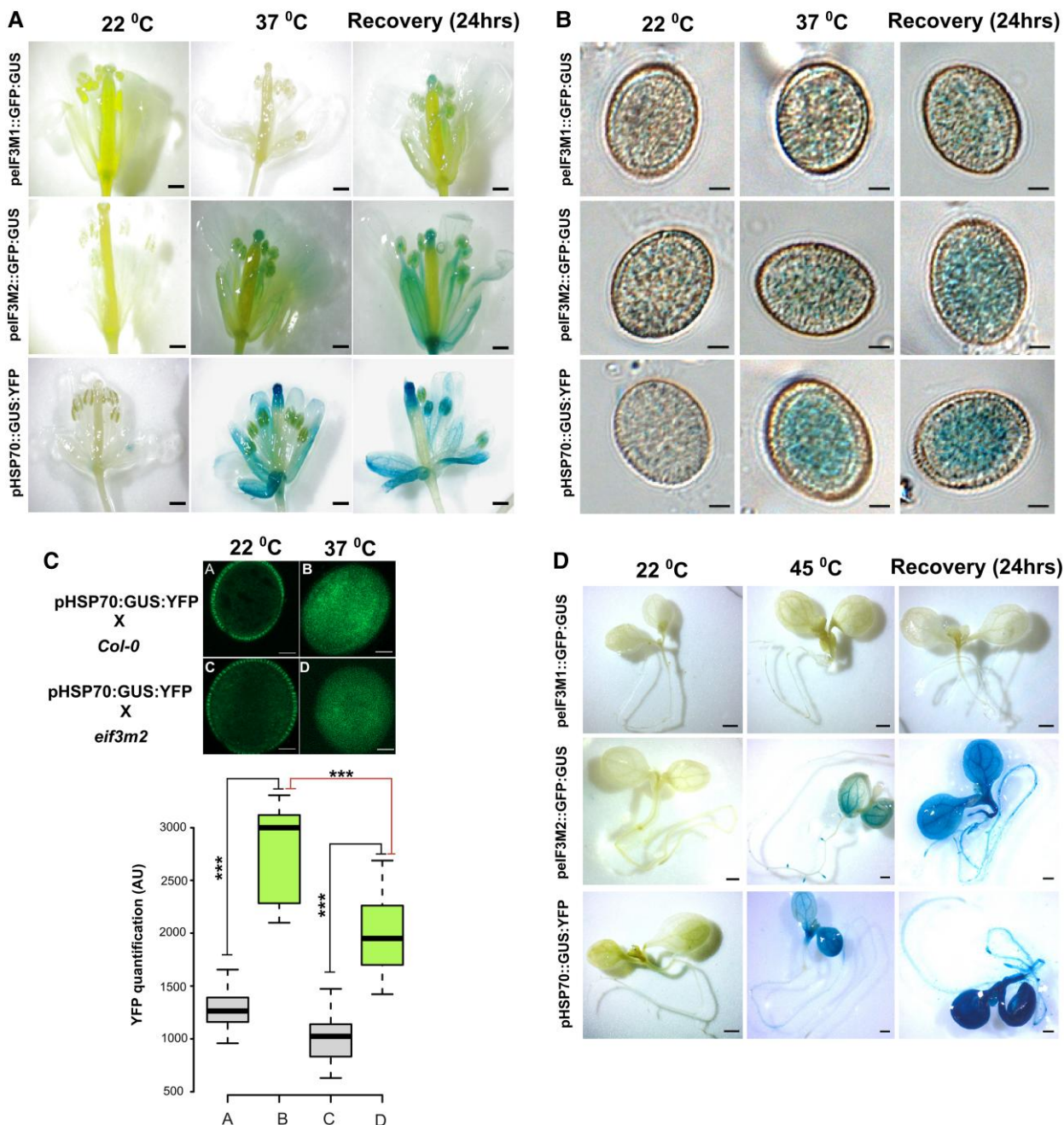


Figure 2. *eIF3M2* and *HSP70.1* promoter activities increase upon heat stress. **A, B)** Histochemical GUS staining of native promoters of *eIF3M1*, *eIF3M2*, and *HSP70.1* promoter::GFP:GUS fusion in open flowers and mature pollen grains in control conditions at 22 °C, under HS at 37 °C, and 24 h post HS recovery. Scale bars: **A)** 1 mm and **B)** 5 μ m. **C)** Box plot showing YFP signal quantification of *HSP70* promoter::GUS:YFP activities in mature pollen from *Col-0* and heterozygous *+eif3m2* mutant background. Center lines show the medians; box limits indicate the 25th and 75th percentiles as determined by R software; whiskers extend 1.5 times the interquartile range from the 25th and 75th percentiles; and asterisks represent statistical differences measured by Student's t test: ****P* < 0.01, *n* = 76. Scale bar: 5 μ m. **D)** Similar promoter analysis was performed in 8-d-old seedlings and revealed similar upregulation response of *eIF3M2* and *HSP70* promoters to HS. Scale bar: 1 mm.

Since we observed reduced levels of *HSP70.1* in *eif3m2* mutant background (Fig. 1), we tested *HSP70.1* promoter activity in *eif3m2* mutant background to establish whether the reduced *HSP70.1* expression is associated with reduced *HSP70.1* promoter activity following *eif3m2* loss of function. We therefore quantified the YFP signal of the *HSP70* promoter line (p*HSP70.1::GUS::YFP*) in wild type and in *eif3m2* mutant background. Specifically, we analyzed mature pollen YFP fluorescence intensity under control condition at 22 °C and under HS condition at 37 °C to determine the effect of the *eif3m2* mutation on *HSP70.1* promoter expression. Our observations revealed decreased levels of YFP signal predominantly at 37 °C when the *HSP70* promoter was in the +*eif3m2* mutant background compared to the control wild-type Col-0 background (Fig. 2C). This reduction in YFP signal under the HS conditions suggests that the *eif3m2* mutation negatively affects the activation of the *HSP70.1* promoter activities, inferring that *eIF3M2* acts as a potential regulator of *HSP70.1* enhanced transcriptional activation during HSR (Fig. 2C).

Overexpression of eIF3M2 leads to higher HSP70 expression levels

So far, we observed that knockdown of *eif3m2* reduces the expression levels of *HSP70.1*, whereas knockdown of *eif3m1* (which induces transcriptional upregulation of *eIF3M2* expression) upregulated *HSP70.1* expression during HSR and during HS recovery

(Figs. 1 and 2). Moreover, both *eIF3M2* and *HSP70.1*, but not *eIF3M1*, promoter activities increased during HS and upon recovery (Fig. 2). To further elaborate if *eIF3M2* has a role on *HSP70.1* abundance, we overexpressed both *eIF3M1* (*eIF3M1::YFP*) and *eIF3M2* (*eIF3M2::YFP*) using a pollen vegetative cell-specific promoter, *LAT52*, and repeated the HS experiment with in vitro grown PTs. Our results showed that higher levels of *eIF3M2* directly correlated with increased abundance of *HSP70* levels, both at the RNA and the protein level during HS (Fig. 3, A to E). On the contrary, increased levels of *eIF3M1* had no contributing effect on *HSP70.1* expression and was comparable to *HSP70* expression levels when coexpressed with the control *pLat52::YFP* (Fig. 3, B and D). We conclude that even though *HSP70.1* expression levels are already induced by HS, overexpressing *eIF3M2* followed by HS elevates *HSP70* expression levels even more, suggesting a direct relationship between *eIF3M2* and *HSP70* expression during HSR.

Under the control conditions, *eIF3M1* and *eIF3M2* promoter GUS expression was detected in pollen developmental stages and mature ovules of Arabidopsis (Supplementary Fig. S4, A to C). In stable overexpression line *pLat52::eIF3M2::YFP*, *eIF3M2* localized to the vegetative cell nucleus and the cytoplasm of Arabidopsis pollen and PTs (Supplementary Fig. S4, D to F). Under the HS conditions at 42 °C for 3 h however, the *eIF3M2::YFP* relocalized into large cytoplasmic punctates with increased fluorescence intensity compared to the signal under control conditions (Fig. 3C). In contrast, *eIF3M1*:

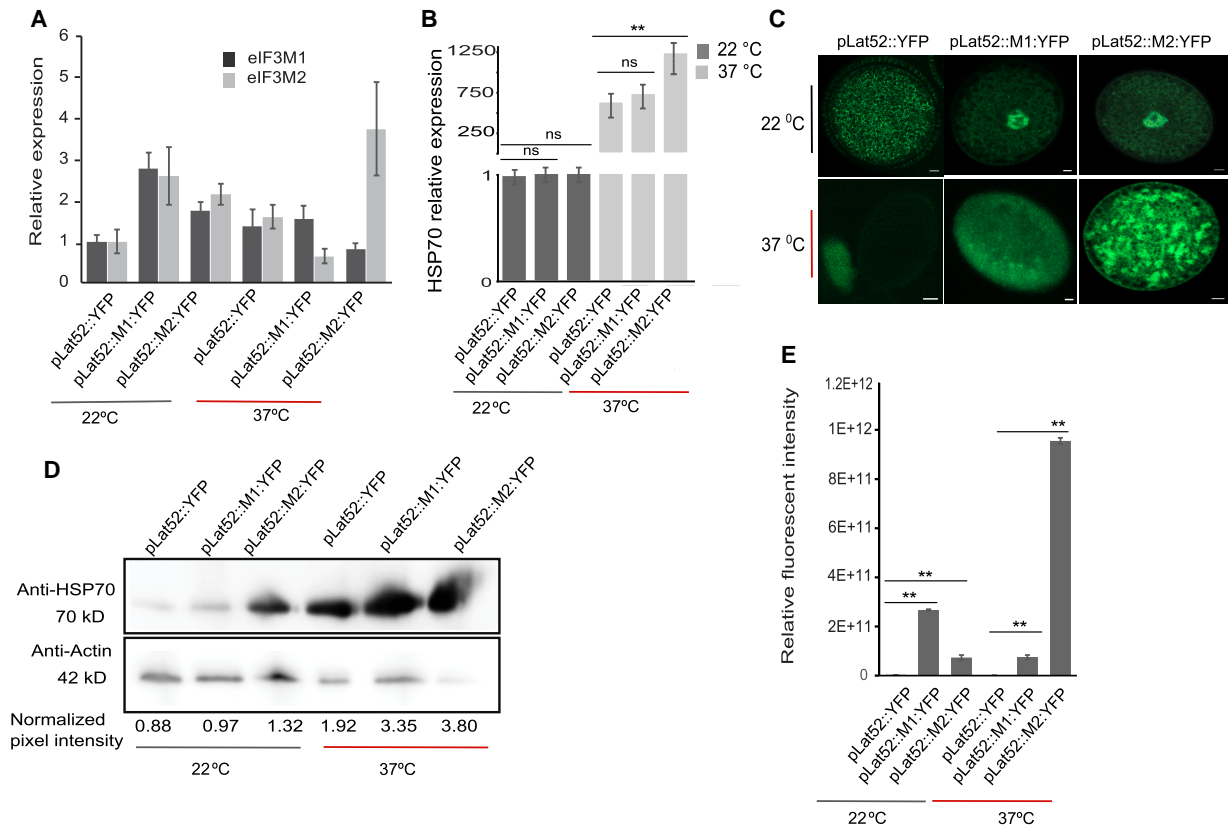


Figure 3. Increased *HSP70* levels are associated with higher levels of *eIF3M2* in PT. **A, B**) qPCR analysis of *eIF3M1*, *eIF3M2*, and *HSP70* in *eIF3M1::YFP* and *eIF3M2::YFP* overexpression lines under the control and HS conditions. Data values were normalized to *pLat52::YFP* levels at 22 °C. **C**) Fluorescent intensity before and after HS in *eIF3M1::YFP* and *eIF3M2::YFP* overexpression lines in pollen. Scale bar: 2 μm. **D**) *HSP70* protein level in *eIF3M1::YFP* and *eIF3M2::YFP* overexpression lines under the control and HS conditions. Pixel intensities were measured with ImageJ plugin and normalized to each corresponding actin band. **E**) Quantification of YFP relative intensity. Signals were normalized to *pLat52::YFP* control. Data are means (±SD, n = 3 replicates). Statistical differences compared with the Col-0 were determined using Student's t tests: **P < 0.01, ns: not significant difference. Same statistical approach was applied to all comparisons shown in this figure.

YFP signal diminished under HS conditions and did not show much significant relocalization (Fig. 3E). These results suggest that unlike eIF3M1, eIF3M2 strongly responds to HS at transcriptional and translational levels and undergoes protein conformational changes and relocalization.

Higher eIF3M2 levels preserve PT membrane integrity upon HS

The correlation between eIF3M2 and the HSP70 expression levels upon HS prompted us to hypothesize that higher levels of eIF3M2 would impose better HSR and PT resilience under HS. To test our hypothesis, we set up an in vitro pollen germination experiment to first understand how eIFM1 and eIFM2 overexpression affected pollen germination and PT growth under normal control conditions. At 22 °C, both eIF3M1:YFP and eIF3M2:YFP overexpression lines germinated poorly (36.4% and 32.2%, $n > 350$) and showed a higher ratio of burst germinating pollen and PTs (Fig. 4, A to C). Some of the germinated PTs showed branching phenotype that later burst (Fig. 4C). However, under HS conditions, at 37 °C for 2 h followed by 2 h at 22 °C, control overexpression lines, pLat52:YFP, and eIF3M1:YFP overexpression and native eIF3M1:mCherry performed worse showing higher degree of ungerminated pollen and burst PTs (27.6% and 62.2%, respectively, $n = 389$) than in control conditions (Fig. 4B). In contrast, native eIF3M2:YFP as well as the overexpression line pLat52:eIF3M2:YFP sustained better the HS and showed better pollen germination rate (42.6% and 55.9%, $n = 332, 413$), reduced PT branching (2.3% and 4.6%, $n = 332, 413$), and showed reduced PT burst (31.3% and 23.2%, $n = 332, 413$) (Fig. 4B). Altogether, our observations link the higher expression

levels of eIF3M2 with increased expression of HSP70 to increase PT robustness and integrity upon HS exposure and therefore better thermotolerance potential.

The eIF3M2-HSP70 module action for HS tolerance extends to the sporophyte

To understand if the HS response of eIF3M2 and HSP70 coregulation is gametophytic specific, we analyzed heat tolerance of 8-d-old seedlings expressing native *peIF3M1::eIF3M1:mCherry* and *peIF3M2::eIF3M2:mCherry* constructs. Seedlings were first primed to HS at 38 °C for 90 min, then transferred back to control condition at 22 °C for 2 h followed by 3 h HS at 45 °C. We then measured global translational changes by polysome profiling as well as monitored HSP70 translational efficiency. Under the control conditions at 22 °C, there were no differences between eIF3M1:mCherry and eIF3M2:mCherry transgenic lines with the wild-type Col-0 control (Fig. 5, A to D). Under the HS conditions however, we detected a reduction in polysome-to-monosome ratio in wild-type Col-0 and eIF3M1:mCherry transgenic seedlings suggesting global translation reduction, whereas eIF3M2:mCherry seedlings maintained almost 50% of its original translation rate observed under the control conditions (Fig. 5B). Analysis of HSP70 RNA and protein levels showed increase of HSP70 expression under HS conditions in wild-type Col-0 and in eIF3M1:mCherry seedlings; however, HSP70 expression levels were more elevated in eIF3M2:mCherry transgenic seedlings under HS conditions (Fig. 5, C and D). Our results support that the eIF3M2-HSP70 HSR module is not exclusive to the male gametophyte but it is also conserved in the sporophyte.

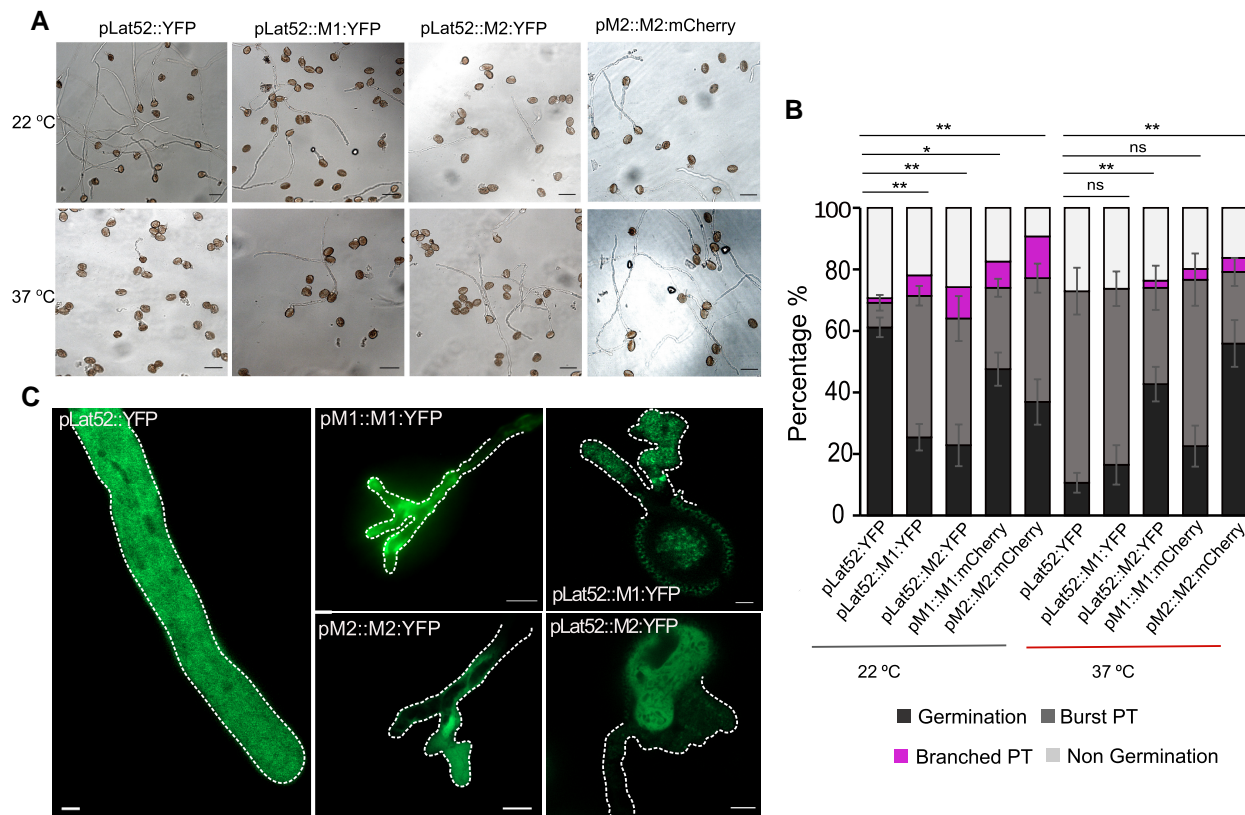


Figure 4. Higher eIF3M2 levels maintain PT integrity upon HS. **A, B)** PT germination of eIF3M1:YFP and eIF3M2:YFP overexpression lines and native lines under control condition (6 h at 22 °C) and under HS condition (2 h at 22 °C and 4 h at 37 °C); $n > 350$. Scale bar: 50 μm . **C)** Normal PT, branched, and burst PT phenotypes of eIF3M2:YFP overexpression lines under normal condition. Scale bar: 5 μm . Data are means (\pm SD). Significant differences compared with the Col-0 were determined using Student's *t* tests: ** $P < 0.01$, * $P < 0.05$, ns: not significant difference.

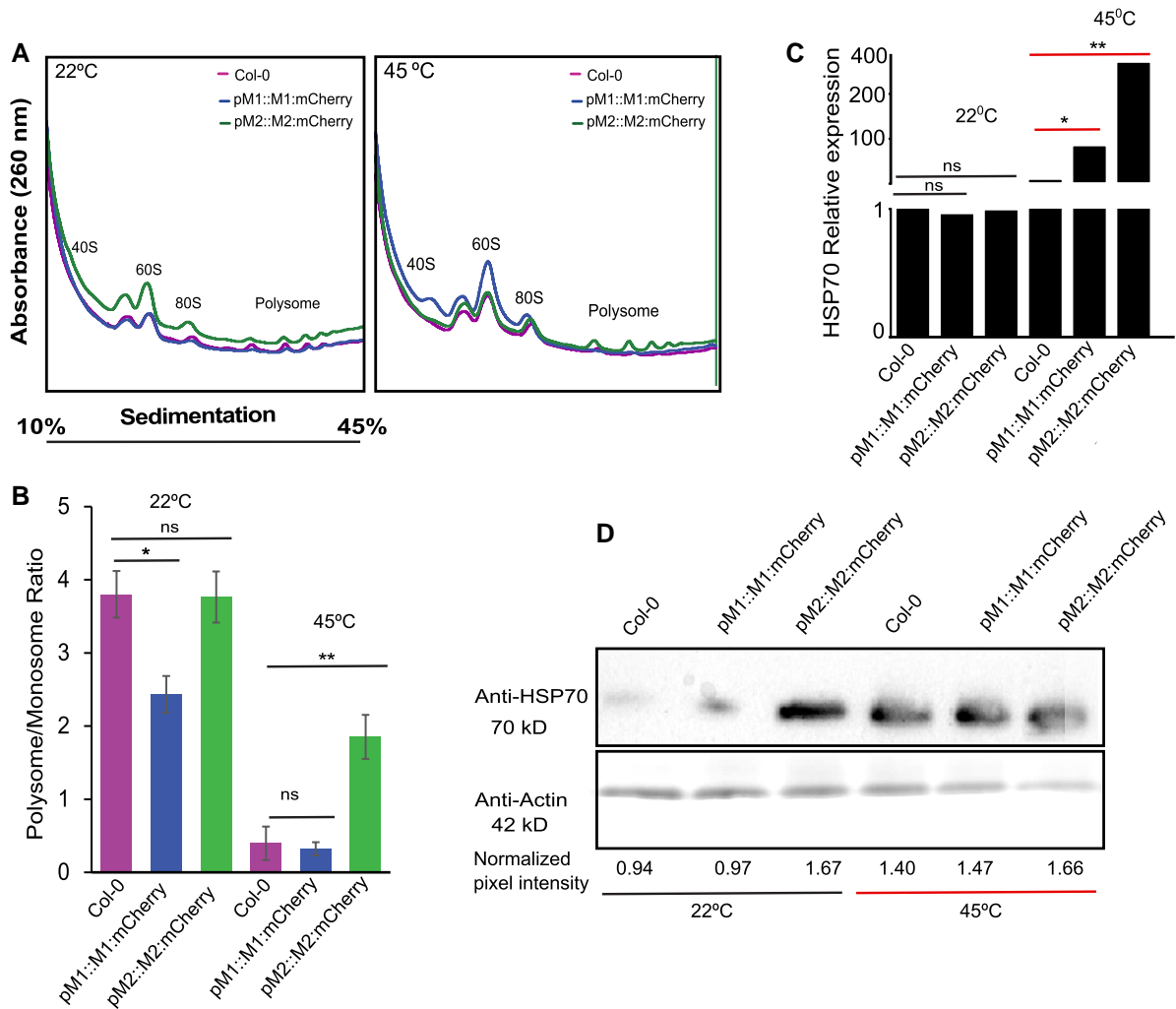


Figure 5. eIF3M2-HSP70 relationship is maintained in the sporophyte and leads to higher translation efficiency under HS. **A)** Polysome profiles of eIF3M1 and eIF3M2 driven by native promoter in comparison with Col-0 under control and HS conditions performed with 8-d-old seedlings in triplicates. Polysome profiles were generated following fractionation on a 10% to 45% sucrose gradient. Peaks corresponding to 40S subunits, 60S subunits, and 80S ribosomes are labeled, and the locations of polysomes are indicated. **B)** Difference in polysome to monosome ratio in Col-0, proeIF3M1::M1:mCherry, and proeIF3M2::M2:mCherry lines in Col-0 background under control and HS conditions. **C)** HSP70 transcript level in Col-0, proeIF3M1::M1:mCherry, and proeIF3M2::M2:mCherry lines in Col-0 background under control and HS conditions. **D)** HSP70 protein level in Col-0, proeIF3M1::M1:mCherry, and proeIF3M2::M2:mCherry lines in Col-0 background. Pixel intensities were measured with ImageJ plugin and normalized to corresponding actin band. Data are means (\pm SD, $n = 3$ replicates). Statistical differences compared with the Col-0 were determined using Student's *t* tests: ** $P < 0.01$, * $P < 0.05$, ns: not significant difference. Same statistical approach was applied to all comparisons shown in this figure.

The eIF3M2-HSP70 HSR in Arabidopsis is maintained in *N. tabacum* PTs

We next questioned whether the eIF3M2-HSP70 HSR relationship is unique to Arabidopsis or if it can have a wider evolutionary implication. We therefore generated stable *N. tabacum* transgenic lines expressing pLat52::AtelF3M2:YFP and repeated our HS experiments. Similar to our observations in Arabidopsis, AtelF3M2:YFP localized to tobacco PT cytoplasm and to the nucleus under normal conditions, showed reduced tobacco pollen germination, and increased expression levels of native tobacco HSP70 (Fig. 6, A to D). When we subjected the tobacco PTs to HS at 42 °C for 3 h, both AtelF3M2:YFP and HSP70 expression levels increased significantly compared to their expression under normal growth conditions and showed improved pollen germination compared to the control pollen expressing YFP alone (Fig. 6, A to D). Moreover, after the 3 h HS, the cytoplasmic subcellular localization of AtelF3M2:YFP shifted into cytoplasmic protein punctate, similar to the response

we observed in Arabidopsis pollen (Fig. 6A). Western blot analysis using anti-HSP70 antibodies confirmed the increased levels of HSP70 upon HS exposure in PTs (Fig. 6D). When we analyzed global translation by polysome profiling in PTs, we detected a slight increase in translation efficiency in AtelF3M2:YFP overexpression lines as indicated by higher polysome-to-monomer ratios (Fig. 6, E and F). Collectively, our findings in tobacco PTs imply that the eIF3M2-HSP70 relationship during HSR could be a universal mechanism across different plant species particularly in flowering plants.

eIF3M2 coimmunoprecipitates and directly interacts with cytoplasmic HSP70 and eIF4G

To gain insight into the relationship between eIF3M2 and HSP70 in PTs, we tested next whether eIF3M2 could also associate with HSP70 through protein-protein interaction. We germinated in vitro tobacco PTs under standard conditions expressing eIF3M2:YFP and control PTs expressing YFP tag alone both under the Lat52

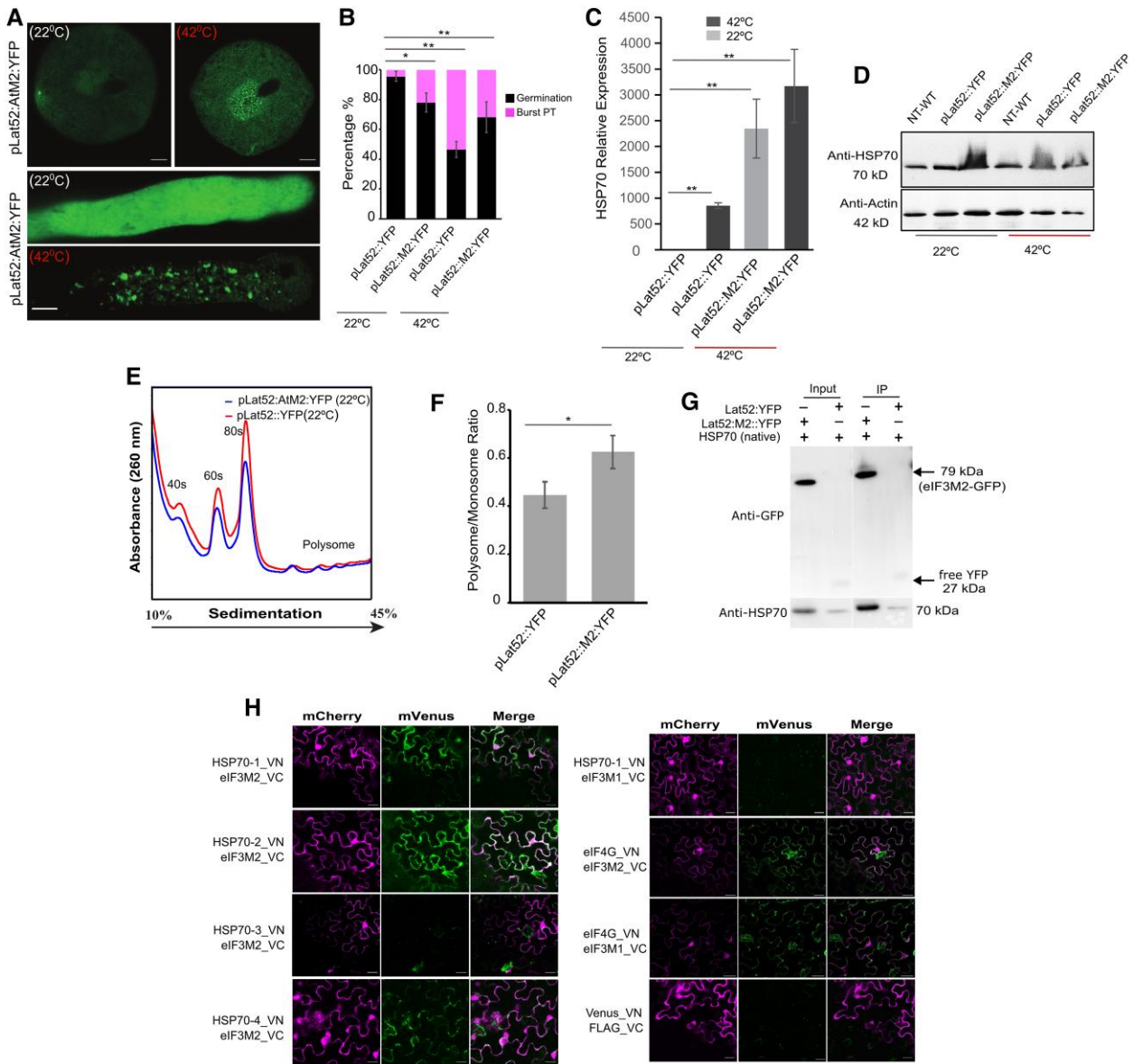


Figure 6. eIF3M2 directly interacts with cytoplasmic HSP70 and eIF4G. **A, B** Subcellular localization of eIF3M2 in *N. tabacum* mature pollen and in vitro PT under control and HS condition and efficiency of in vitro PT germination of the corresponding lines ($n = 271$). Scale bar: 5 μm. **C** HSP70 transcript level in AtelF3M2 overexpression lines driven by Lat52 promoter in comparison with pLat52::YFP lines ($n = 3$ replicates). **D** HSP70 protein levels in eIF3M2 overexpression lines. **E** Polysome profiles of eIF3M2 overexpression lines in tobacco PTs. Polysome profiles were generated following fractionation on a 10% to 45% sucrose gradient. Peaks corresponding to 40S subunits, 60S subunits, and 80S ribosomes are labeled, and the locations of polysomes are indicated. **F** Difference in polysome to monosome ratio in control lines and eIF3M2 overexpression lines in *N. tabacum* PTs ($n = 3$ replicates). **G** eIF3M2 coimmunoprecipitates with HSP70 under normal condition. **H** Verification of eIF3M2-HSP70-eIF4G interaction by the BiFC method. Split Venus (mVenus-N-terminal, V [210aa] and FLAG-mVenus-C-terminal, VC [30aa]) constructs were expressed in *N. benthamiana* leaf epidermal cells to validate direct protein-protein interaction between HSP70 paralogs and eIF4G with eIF3M2. mVenus-N-FLAG::mVenus-C and eIF3M1-HSP70-1 interactions were used as negative controls. Scale bar: 20 μm. Data are means (\pm SD, $n = 3$ replicates). Statistical differences compared with the Col-0 were determined using Student's *t* tests: ** $P < 0.01$, * $P < 0.05$. Apply to all comparisons shown in this figure.

promoter. Following affinity immunoprecipitation with anti-GFP agarose resin trap (Chromotek), both eIF3M2:YFP and YFP tag could be captured and were both detected by western blot using anti-GFP antibody (Fig. 6G). Interestingly, PTs expressing eIF3M2:YFP strongly coimmunoprecipitated with HSP70 suggesting that eIF3M2 associates with HSP70 in PTs via protein-protein interaction (Fig. 6G). To validate this potential association, we next investigated direct interaction between eIF3M2 and 4 cytoplasmic HSP70s in Arabidopsis expressed in pollen, HSP70.1, HSP70.2, HSP70.3, and HSP70.4 (AT5G02500, AT5G02490, AT3G09440, and AT3G12580), using bimolecular fluorescence complementation

(BiFC) assay with split mVenus. In addition, since eIF4G was shown to alleviate HS by promoting the translation of HS-related mRNAs via eIF4A mRNA recruitment in yeast (Desroches Altamirano et al. 2024), we also tested possible interaction between eIF3M2 with eIF4G as an additional module of eIF3M2 promoted thermotolerance. Our results showed that eIF3M2 interacts with HSP70.1, HSP70.2, and HSP70.4 in the cytoplasm but not with HSP70.3 in tobacco leaf epidermal cells (Fig. 6H). As a control, we show that eIF3M1 does not show a similar interaction with HSP70.1 (Fig. 6H). Additionally, we verified that eIF3M2 also directly interacts with eIF4G (Fig. 6H).

Collectively, these findings imply that eIF3M2-HSP70-eIF4G could coassociate in a common complex through protein-protein interaction as a module for HS thermotolerance in flowering plants.

Higher eIF3M2 and HSP70.1 levels reduce ROS accumulation to maintain PT membrane integrity

To determine the mechanism through which the eIF3M2-HSP70 module maintain PT integrity under HS condition, we overexpressed NtHSP70.1:YFP and AteIF3M2:YFP in tobacco PTs and subjected the PTs to HS. We applied a VAHEAT precision chip (Interference GmbH) mounted on the slide for the induction of HS on PT and used confocal high-resolution microscopy for time course live cell imaging to monitor PT morphology under differential interference contrast (DIC), YFP protein subcellular dynamics

and simultaneous production of ROS using CellROX dye (Thermo Fisher). Upon HS induction at 42 °C, PT expressing control Lat52:YFP was observed to start to deform within 1.5 min of HS application, accumulated YFP protein aggregates and high levels of ROS, and within 7 min the PT completely lost integrity and burst (Fig. 7, A to C). In contrast, no deformation was visible in PT overexpressing eIF3M2:YFP, and the eIF3M2 protein remained localized in the cytoplasm without much aggregation even after 7 min of HS (Fig. 7, A and B). Only after 24 and 35 min, some of the eIF3M2:YFP PT showed swollen tip, cytoplasmic retraction, initiated small cytoplasmic protein punctates but importantly maintained low levels of ROS, strongly demonstrating that by retaining low ROS levels, eIF3M2 can maintain PT integrity during HS (Fig. 7, B and C). We obtained similar results when we overexpressed NtHSP70.1:YFP, where PT integrity was also maintained even after

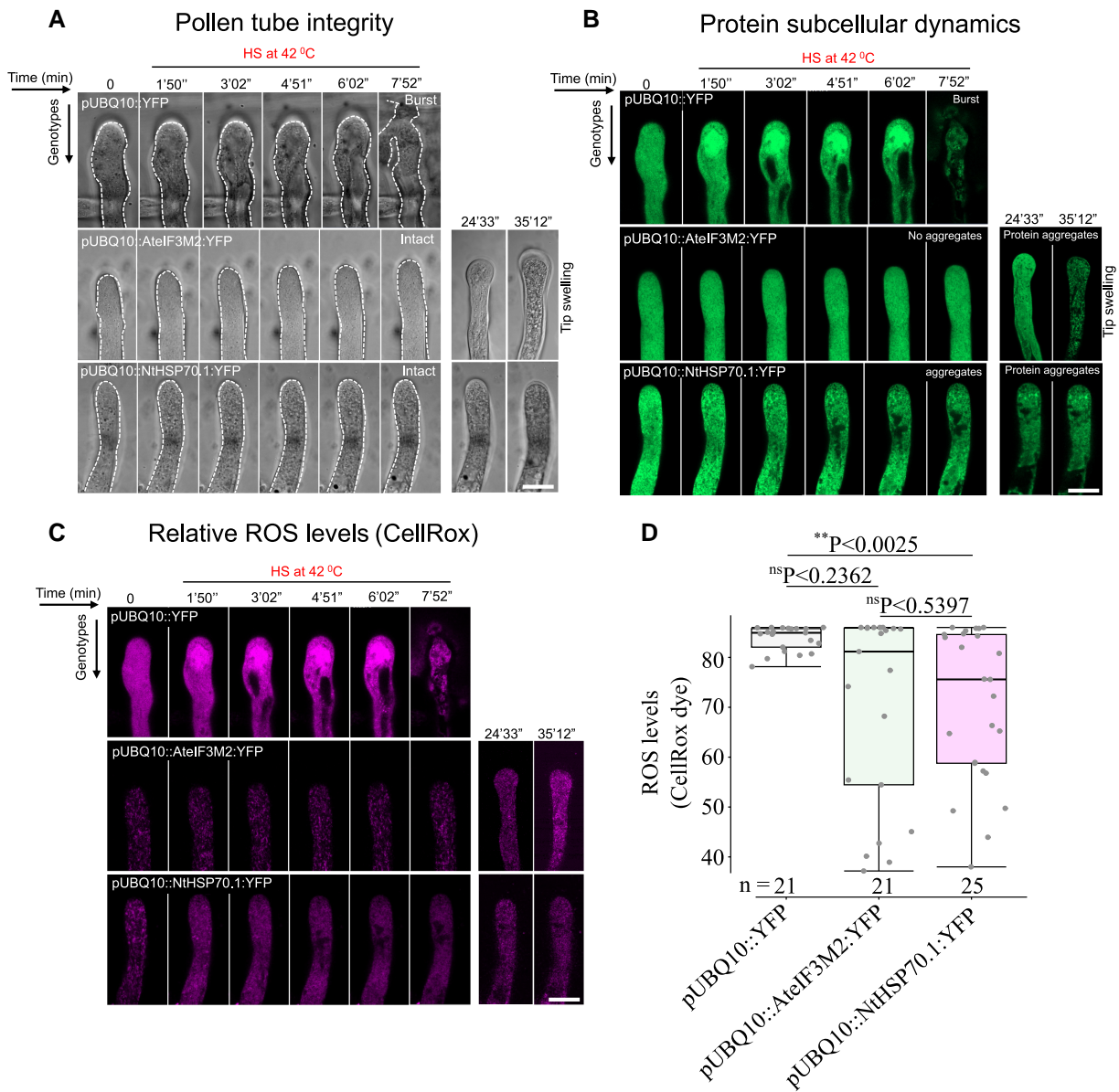


Figure 7. eIF3M2-HSP70 overexpression reduces ROS accumulation to maintain PT integrity. **A to C)** VAHEAT precision on-slide chip HS induction was performed with tobacco PTs expressing control pLat52::YFP, pLat52::AteIF3M2:YFP, and pUBQ10::NtHSP70.1:YFP. High-resolution confocal LSM900 was used for live cell imaging to simultaneously record PT behavior under DIC optics. **D)** YFP detection for protein subcellular changes and measurement of ROS levels using CellROX staining of the PTs. PTs were analyzed 8 h after particle gene gun transformation. Center lines show the medians; box limits indicate the 25th and 75th percentiles as determined by R software; and whiskers extend 1.5 times the interquartile range from the 25th and 75th percentiles. Sample size, $n = 67$ (at least 3 replicates performed). Scale bar: 10 μm for all panels.

35 min of HS at 42 °C (Fig. 7, A and C). However, unlike AteIF3M2, NtHSP70.1:YFP generated protein punctates within a minute of HS application and the punctates steadily increased in size with time (Fig. 7B). Similar to eIF3M2, NtHSP70.1:YFP overexpression also showed low levels of ROS accumulation even after 35 min of HS application (Fig. 7C). Quantification of the CellROX dye revealed that on average there were 10x more ROS levels in the YFP control PT than in eIF3M2 or NtHSP70.1 overexpressing PTs (Fig. 7D). These results directly link suppression of ROS accumulation in eIF3M2 or NtHSP70.1 overexpression in PT as a mechanism to maintain PT integrity upon HS exposure.

Discussion

Temperature is currently the most destructive environmental factor affecting plant reproductive processes such as pollen germination, PT growth, and fruit set, more so relevant at the current global rise in climate temperature. In this study, we have identified a link between the eIF3M2 translation initiation subunit of the eIF3 complex as a developmental regulator for male gametogenesis and as a positive trait for thermotolerance. Our results, combining analysis of genetic mutants and overexpression experiments, support that eIF3M2 imposes upregulation of HSP70 to maintain PT integrity under HS conditions, and therefore, a positive selection trait for reproduction adaptation of crops under high temperature changes. Exposure to HS reduces in vitro pollen germination and PT growth in almost all crops including wheat, rice, and maize as well as affecting fruit setting of several plant species such as tomato (Jiang et al. 2017). For a cell to endure stress, it is essential to maintain cellular protein configuration, low oxidative toxicity, and reduce cellular sensitivity to stress. HSPs facilitate protein refolding and stabilize polypeptides and membranes under stress conditions. In particular, HSP70 plays a critical role as a chaperone in preventing protein aggregation and assisting protein refolding of nonnative conformation under stress conditions and upon HS recovery (Usman et al. 2017).

In Arabidopsis, in vitro pollen germination has been reported to be sensitive to temperatures at 28 and 37 °C (Rodriguez-Enriquez et al. 2013). In our study, HS of *eif3m2* mutants at 37 °C decreased the rate of pollen germination in vitro and increased the rate of PT burst (Fig. 1). In contrast, we observed increased pollen germination rate in *eif3m1* mutants under HS at 37 °C compared to at 22 °C. Our findings in this study propose that this increase of *eif3m1* pollen germination rate can be explained by the higher levels of eIFM2 and HSP70 expression in *eif3m1* mutant background (Fig. 1). In support, under HS conditions, eIF3M2 overexpression lines also had a higher germination ratio and a lower rate of burst and branched PTs, which was also associated with higher levels of HSP70 expression (Fig. 4; Parotta et al. 2013, 2019). Indeed, HSP70 expression levels substantially increased in eIF3M2 overexpression lines under control and HS conditions (Figs. 1 to 3). Moreover, we observed that the HS increased eIFM2 and HSP70 promoter activities but not that of eIF3M1 (Fig. 2). This differential response between eIF3M1 and eIF3M2 subunits to HS and the positive correlation between eIF3M2 and HSP70 coordinated response to HS appeared not to be exclusive to the male gametophyte but also conserved in the sporophyte of Arabidopsis. We tested this conserved regulation in the sporophyte using native promoters driven eIF3M1:mCherry and eIF3M2:mCherry on 8-d-old seedlings exposed to HS at 45 °C. When compared to Col-0, the global translation efficiency assessed by monitoring polysome accumulation was significantly higher in eIF3M2:mCherry lines and further correlated with the increased accumulation of HSP70 mRNA and

protein levels in eIF3M2:mCherry background (Fig. 5). Altogether, our data support a mechanism involving a coordinated response between eIF3M2 and HSP70 to protect plants from adverse HS.

To draw analogy, HSP70 interacts with eIF4G to stimulate protein synthesis, increase cell proliferation, and reduce cell death under hypoxia stress (Wang et al. 2020). In yeast, eIF4G promotes HS-related mRNA translation through eIF4A-selective mRNA recruitment to improve yeast survival upon HS (Altamirano et al. 2024). We have shown here that eIF3M2 directly interacts with eIF4G in *Nicotiana benthamiana* pavement cells (Fig. 6). We can therefore extrapolate that by directly associating with eIF4G, eIF3M2 might aid in the recruitment and enhanced translation of HS-related mRNA via eIF4G to promote thermotolerance in PT upon HS. Indeed, depletion of *eif3m2* alone strongly abolishes thermotolerance in PTs (Fig. 1).

It has also been shown that cytoplasmic protein aggregation and the accumulation of misfolded proteins trigger reductive stress (Lin et al. 2020). In this study, we have shown that eIF3M2 coimmunoprecipitates with HSP70 in PTs and that eIF3M2 directly interacts with HSP70.1, HSP70.2, and HSP70.4 in *N. benthamiana* leaf pavement cells (Fig. 6). Moreover, we observed that upon HS, eIF3M2:YFP and NtHSP70.1:YFP form cytoplasmic protein aggregates in PTs (Figs. 6 and 7). We attempted to colocalize these aggregates formed by eIF3M2 and HSP70.1; however, cooverexpression of both of these proteins proved to be lethal to PT germination. Nevertheless, the interaction between eIF3M2-HSP70 could likely reduce accumulation of misfolded proteins and reduce cellular stress induced by the HS as one possible mechanism (Figs. 3 and 6). To protect cells from reductive stress, we have shown that overexpression of either eIF3M2 or HSP70.1 strongly reduces ROS accumulation in tobacco PTs (Fig. 7). The reduction of ROS accumulation prevents PT from osmotic burst as seen with the control PT (Fig. 7). We therefore infer that eIF3M2 mediates thermotolerance and protects PT integrity under the HS conditions by upregulating HSP70 expression levels to mitigate unfolded protein accumulation and directly interact with HSP70 and eIF4G to promote hypertranslation of HS-related mRNAs (Fig. 8).

Several other studies have reported the involvement of other plant eIFs in abiotic stresses. Overexpression of eIF1A improved tolerance to salt stress (Rausell et al. 2003), whereas overexpression of eIF5A increased resistance to osmotic, nutrient, oxidative, and high-temperature stresses (Xu et al. 2011). Interestingly, a mutation in eIF5B1 is responsible for the *hot3-1* thermotolerance defect by interfering with the interactions and mechanism of gene-specific translational control (Zhang et al. 2017). Thus, specific manipulation of translation initiation factors may represent a credible approach to improve plant survival under abiotic and biotic stresses.

Similar to the vegetative tissues, in vitro germinated Arabidopsis pollen responds to extreme stress conditions by upregulating HS genes. Correlation between transcriptional and translational responses to high temperatures was revealed by ribosome profiling in conjunction with RNA-seq and specific mRNA translational regulation (Poidevin et al. 2021). In tomato pollen, HsfA2 regulates a subset of HS-induced genes (including several HSPs) and functions as an essential coactivator of HsfA1a during the HSR (Fragkostefanakis et al. 2016). In Arabidopsis and tobacco pollen, our study unveils a previously unknown link between translation initiation subunit eIF3M2 and HSP70 as a core module that buffers HS in PT, maintaining PT membrane integrity and prevents PTs from premature burst. eIF3M2 not only stimulates HSP70 accumulation, but we show that eIF3M2 likely forms a complex with HSP70 and eIF4G in tobacco PT as verified by direct

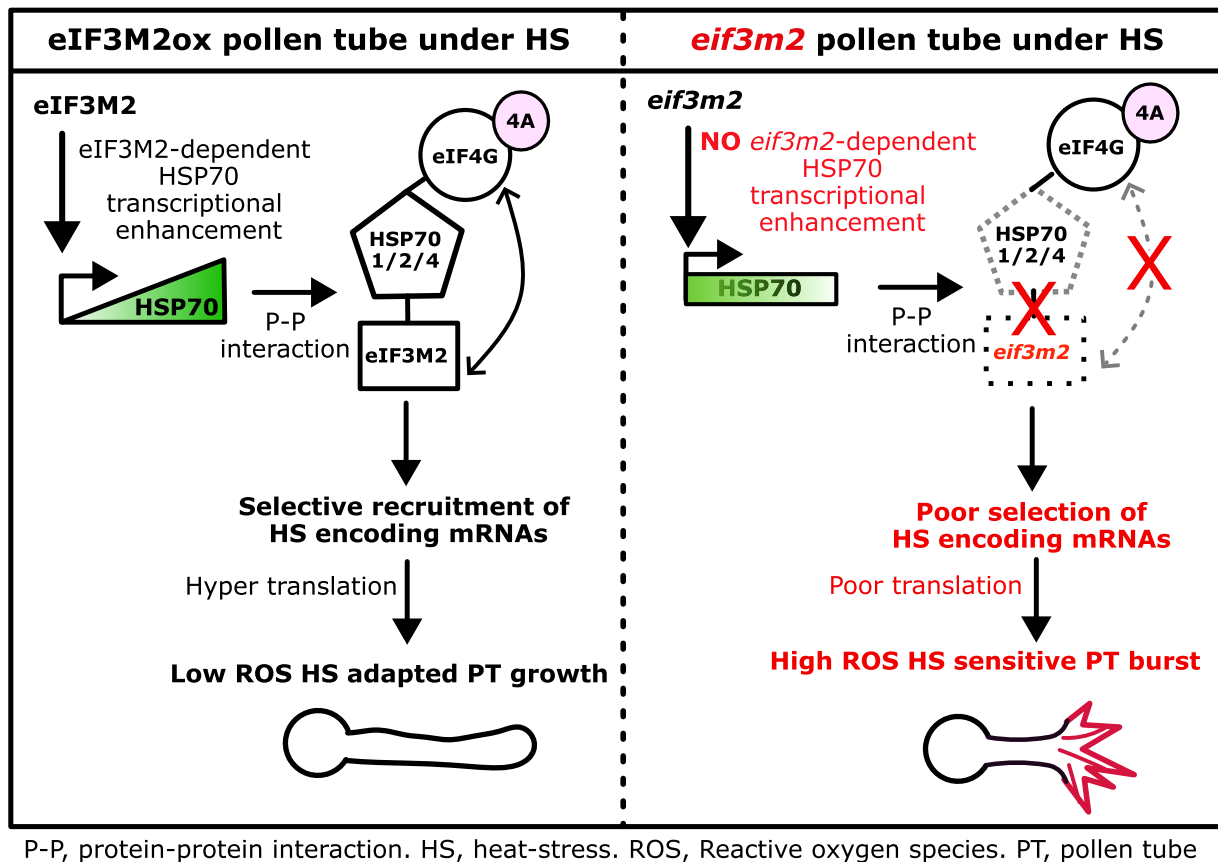


Figure 8. A representative working model of eIFM2-HSP70-eIF4G module during Arabidopsis PT growth under HS conditions. *oxeIF3M2*, overexpression of eIF3M2 in PT. The triangle labeled HSP70 represents higher levels of HSP70, whereas the rectangle represents decreased levels of HSP70. The dashed lines represent weak or no interaction.

protein-protein interaction in leaf pavement cells (Figs. 6 to 8). These results imply that eIF3M2-HSP70-eIF4G functions as a module through protein-protein interaction likely with other cofactors to enforce thermotolerance and protect PT integrity during HS. It will be very interesting to investigate if overexpression of HSP70 can directly rescue the PT burst phenotype of *eif3m2* mutant under the HS conditions to understand the hierarchy of the eIF3M2-HSP70 thermotolerance module.

Conclusion

In summary, our findings conclude that the eIF3M2-HSP70-eIF4G module plays a crucial role in maintaining PT integrity under HS conditions. This protective mechanism and thermotolerance involve higher expression levels of eIF3M2, which directly enhances abundance of HSP70 HS chaperone protein at both the mRNA and the protein level, and that eIF3M2 physically interacts with HSP70.1, HSP70.2, HSP70.4, and eIF4G (Figs. 6 and 8) to reduce cellular stress associated with unfolded protein response and ROS accumulation to maintain PT integrity.

Materials and methods

Plant materials and growth conditions

T-DNA insertion lines were obtained from the Arabidopsis Biological Resource Center (www.arabidopsis.org): *eif3m1-1* (SAIL_184_H06), *eif3m1-2* (SALK_seq_087061.1), *eif3m2-1* (SALK_003895), and *eif3m2-2* (SALK_151350). The T-DNA lines were genotyped with LBb1.3 or SAIL LB2 primers alongside

gene-specific primers (Supplementary Table S1). For plant growth, seeds were first germinated on 1/2 MS medium with 1% (w/v) sucrose and 0.8% (w/v) agar (Murashige and Skoog 1962). After 8 d, the seedlings were transplanted into soil. Plants were grown in a long-day routine at 22 °C for 3 to 4 wk. Floral dipping was done according to Clough et al. (1998), and transformed plants were selected on MS media with appropriate antibiotics and cultivated under standard conditions.

Histochemical GUS staining

pAt $eIF3M1::GFP::GUS$ and pAt $eIF3M2::GFP::GUS$ constructs were transformed into wild-type (Col-0). For both genes, we cloned promoter fragments of 1,000 bp upstream of translation start codon and cloned them to express GFP::GUS reporter fusion (primer sequences are in Supplementary Table S1). At least 12 independent T1 lines were screened, and selected lines were cultivated further until T3 homozygous generation was obtained. GUS activity was detected using 8-d-old seedlings and inflorescences from 35-d-old plants collected from homozygous plants. The tissues were stained using a GUS buffer solution (50 mM sodium phosphate buffer with a pH of 7, 0.2% Triton X-100, 1 mM X-gluc [Thermo Fisher Scientific, Waltham, MA, USA], and 2.5 mM potassium ferricyanide). Samples were subjected to vacuum infiltration for 10 min followed by incubation at 37 °C for 1 h. The samples were subjected to fixation in ethanol at multiple concentrations, 50% for 1 h, 70% for 1 h, and 99.6% for 1 h. Additionally, the samples were subjected to fixation in 50% ethanol for 24 h at 4 °C.

Phenotype analysis

To find out whether pollen nuclei were normal or deficient, DAPI staining was used (Vergne et al. 1987). Pollen of the wild type is classified to have 2 sperm cell nuclei in close alignment with the vegetative nucleus under fluorescent microscope. The screening of mature pollen samples was conducted using a Nikon TE-2000 microscope under bright-field and UV illumination and Zeiss Axiovert 200M (LSM5).

In vitro and in vivo pollen germination

Boavida and McCormick's (2007) protocol method for in vitro PT growth was followed. The pollen germination rate was determined after 8 h of in vitro growth. Tobacco PTs were germinated in SMM-MES media (0.175 M sucrose, 1.6 mM H₃BO₃, 3 mM Ca(NO₃)₂·4H₂O, 1 mM KNO₃, and 23 mM MES, at pH 5.9 adjusted with 1 M KOH). We sterilized the media in a water bath at temperatures of 100 °C for 45 min. After 24 h, we repeated the sterilizing procedure. The medium was stored at 4 °C.

Vector construction and transient transformation of *N. tabacum* pollen

To generate the NtHSP70.1 overexpression construct, a cDNA fragment was amplified using Phusion polymerase (New England Biolabs) and gene-specific primers containing attB sites overhang for gateway recombination (Supplementary Table S1). The amplified fragment was then recombined using Gateway BP Clonase II Enzyme mix (Thermo Fisher Scientific, Waltham, USA) into pDONR221 (Thermo Fisher Scientific, Waltham, USA) to generate entry clones. Subsequently, the overexpression construct was prepared by recombining entry clone modules (Ubiquitin 10 promoter, NtHSP70.1, and YFP for C-terminal fusion) into to expression vector pB7m34GW,0 using Multisite Gateway TM LR Clonase II Enzyme mix (Thermo Fisher Scientific, Waltham, USA) to generate proUBQ10-NtHSP70.1::YFP construct.

For tobacco pollen transformation, mature pollen grains were collected from greenhouse-grown *N. tabacum* before anthesis, harvested and frozen at -20 °C till further use. Pollen was transiently transformed by a helium-driven biolistic gene gun particle delivery system (PDS-1000/He, Bio-Rad), and PT was grown as previously described by Kumar et al. (2024) and Noack et al. (2019). Before bombardment, the gold particles were coated with 2 µg of plasmid DNA carrying gene of interest for each biolistic pollen transformation. For cotransformation studies, 2 µg of each plasmid DNA was mixed either at the ratio of 1:1 or 1:3 before particle bombardment. Samples were imaged 8 h postgermination at room temperature.

Aniline blue staining of in vivo PT growth

We pollinated WT stigmas with pollen derived from WT, *eif3m1* and *eif3m2*, and *eif3m1/eif3m2* double mutant. Pollinated pistils were fixed and stained with aniline blue using the protocol by Mori et al. (2006). After 24 h, the pistils were observed through microscopy under UV light using the DAPI filter. The screening of pollen germination in vivo was conducted with 3 biological replicates, with each replication involving the measurement of at least 9 pistils.

Heat Shock assay

HS on seedlings was performed according to Hong and Vierling (2000) and Zhang et al. (2017). The seedlings were grown for 8 d

on plates under 16/8 h, 22 °C, day/night cycle and were treated at 38 °C for 90 min followed by 2 h at 22 °C and then 3 h at 45 °C.

For PT HS, Arabidopsis PTs were grown for 2 h at 22 °C, according to Boavida and McCormick's (2007) protocol and then transferred to 37 °C for 4 h. Tobacco PTs were grown for 3 h at 42 °C followed by 3 h at 28 °C. For live cell imaging under direct HS conditions, tobacco PTs were grown for 8 h after particle gene gun transformation and were subjected to HS using on-slide VAHEAT precision (Interference) chip mounted on ZEISS LSM 900 with Airyscan module. Images were captured by time series as defined on figure legends.

ROS measurements

For ROS staining in PTs, the oxidative fluorescent dye CellROX Deep Red (Thermo Fisher Scientific, C10422) was used. CellROX was dissolved in DMSO at stock solution of 2.5 mM. After 8 h of PT germination following gene gun transformation, PTs were stained with 2.5 nM CellROX diluted in 1× SMM-MES tobacco PT germination media (0.175 M sucrose, 1.6 mM H₃BO₃, 3 mM Ca(NO₃)₂·4H₂O, 1 mM KNO₃, and 23 mM MES, at pH 5.9 adjusted with 1 M KOH) and incubated in the dark for 15 min at room temperature. Stained samples were imaged with Zeiss LSM900 Airyscan confocal microscope using 488 and 561 argon lasers at 2% intensity (750 gain) and a 40× water immersion objective with the following filter settings in ZEN black software: GFP excitation at 498 nm and emission maxima of 520 nm and mCherry excitation at 536 nm and emission maxima of 617 nm.

Fluorescence quantification was performed on ImageJ version:2.3.0/1.53f. Box-whisker plots were generated using R studio (Version 2022.12.1+364). Asterisks indicate statistical differences calculated using unpaired nonparametric t test in GraphPad Prism 9 with significance (*P < 0.0025) and ns (nonsignificant) using Mann-Whitney U test (scale bar = 10 µm).

RNA extraction and qPCR analysis

The RNeasy Mini Kit (QIAGEN, Valencia, CA, USA) was used to extract total RNA from inflorescence tissue in 4 biological replicates. Isolated RNA was treated with RQ1 RNase-Free DNase I treatment (Promega in Maryland, MD, USA). The NanoDrop One instrument (Thermo Fisher Scientific, Waltham, MA, USA) was used to measure the RNA quantity and quality. The RNA quality was also verified by electrophoresis in a 2% agarose gel. For preparing the cDNA, reverse transcription (RT) was done for 1 h at 42 °C using ImProm-II Reverse Transcription System (Promega, Madison, WI, USA) with an oligo(dT)₂₀ primer. qPCR measurements were performed using GoTaq Q-PCR Master Mix (Promega, Madison, WI, USA) on a Light Cycler 480 (Roche, Basel, Switzerland) with gene-specific primers.

Ct values were normalized according to GAPC1 (At3g04120) and ACT4 (AT5G59370) in Arabidopsis samples. Rbl25 and DKMD were used as a reference gene for *N. tabacum*. All primers are listed in Supplementary Table S1.

Subcellular localization of eIF3M1 and eIF3M2

To detect the subcellular localization of AtelF3M1 and AtelF3M2, we designed an amplification of the coding sequences of AtelF3M1 and AtelF3M2 by using the Golden Braid 3.0 domesticator software (<https://gbcloning.upv.es/tools/domestication/>). We subcloned these sequences into an expression vector containing green and red fluorescent genes (YFP and mCherry) to generate pLat52::AtelF3M1:YFP/mCherry and pLat52::AtelF3M2:YFP/mCherry. pLat52::AtelF3M2:YFP lines were generated in *N. tabacum*

using the leaf disk transformation method. The transformation method was modified following previous approaches using *N. tabacum* leaf disks from 4-wk-old plants (Horsch et al. 1985). *Agrobacterium* cultures containing *plAt52::eIF3M2:YFP* construct and antibiotic markers (kanamycin) were prepared and used to infiltrate leaf disks, which then transferred to callus induction media (1.23 g MS vitamin solution, 6 g sucrose, 2.4 g agar, 0.15 mL BAP, 300 μ L Cefotax [250 mg/mL], and 300 μ L kanamycin [50 mg/mL]) in the dark at 26 °C for 48 h and then transformed to shoot induction media (1.23 g MS vitamin solution, 6 g sucrose, 2.4 g agar, and 60 μ L NAA) for indirect regeneration. The shoots were cut once they reached a minimum length of 3 cm and small leaves start to emerge. These trimmed shoots were then carefully placed into the rooting media (1.23 g MS vitamin solution, 6 g sucrose, and 2.4 g agar). Shoots were incubated for around 4 to 7 wk to build a robust root system. Then, the plantlets were gently taken from the rooting media and transferred to the soil and characterized after 3 to 5 wk.

Images were captured using Zeiss Airyscan laser scanning microscope LSM900 using 488 argon lasers at 2% intensity (800 gain) and a 40x water immersion objective with the following filter settings in ZEN black software: GFP excitation at 498 nm and emission maxima of 520 nm and mCherry excitation at 536 nm and emission maxima of 617 nm. Images were prepared with Adobe Illustrator 2023 (v27). The subcellular localization experiments were performed using at least 3 biological replicates.

Protein extraction and western blot analysis

In vitro PT samples were collected from liquid pollen germination media (Boavida and McCormick 2007). Ten to twenty milligrams of samples was grounded to a fine powder in a cooled mortar. A volume of 250 μ L of extraction buffer comprising 10 mM Tris-HCl (pH 7.8), 150 mM NaCl, 0.5 mM EDTA, 0.5% Na deoxycholate, 0.5% NP-40, 1 mM PMSF, 1 mM DTT, and EDTA-free Protease Inhibitor Cocktail (Roche, Basel, Switzerland) was added, and the samples were further homogenized by repeated pipetting in an up-down motion. Then samples were subjected to centrifugation at 16,000 $\times g$ for 15 min at 4 °C to remove cellular debris. Protein samples were quantified by Bradford assay according to (Pierce Detergent Compatible Bradford Assay Kit, n.d.). For western blot analysis, all the samples were loaded with the same protein quantity. To ensure equal loading, anti-actin antibody (Agrisera 1:10,000, cat: AS132640-) was used as the loading control. Anti-HSP70 (Agrisera, cat: AS08 371) antibodies at a dilution of 1:7,500 were used to detect the protein levels of HSP70. After the incubation period with primary antibodies, the membranes were incubated with anti-rabbit horseradish peroxidase (HRP)-conjugated secondary antibody (Agrisera, cat: AS09602) for a duration of 1 h at room temperature to facilitate visualization using ECL superbright detection system (Promega).

Pull-down assay

In vitro PT samples expressing *eIF3M2:YFP* and *eIF3:YFP* driven by pollen-specific promoter (*plAt52*) were collected (10 and 20 mg) and were grounded into powder in a mortar. A volume of 250 μ L of extraction buffer comprising 10 mM Tris-HCl (pH 7.8), 150 mM NaCl, 0.5 mM EDTA, 0.5% Na deoxycholate, 0.5% NP-40, 1 mM PMSF, 1 mM DTT, and EDTA-free Protease Inhibitor Cocktail (Roche, Basel, Switzerland) was added, and the samples were further homogenized by repeated pipetting in an up-down motion. The samples underwent a 30-min incubation period on ice with pipetting every 10 min, followed by centrifugation at 16,000 $\times g$ for

15 min at 4 °C. The supernatants were transferred to fresh tubes and subjected to immunoprecipitation using GFP-Trap Agarose beads (Chromotek, Munich, Germany) for 4 h at 4 °C in line with the manufacturer's instructions. GFP-Trap Agarose beads (from Chromotek) were equilibrated with wash buffer (10 mM Tris-Cl, 150 mM NaCl, and 0.5 mM EDTA), and the lysate containing the GFP-tagged proteins was incubated with the equilibrated GFP-Trap Agarose beads for 4 h at 4 °C with constant rotation. After the incubation, the beads were washed 5 times with 3 volumes of wash buffer to remove any nonspecifically bound proteins. For LC-MS/MS, direct on-bead trypsin digest was performed followed by LC-MS/MS peptide sequencing. For SDS-PAGE and western blot, GFP agarose beads were mixed with 3 volumes of SDS-PAGE loading buffer (250 mM Tris-HCl [pH 6.8], 8% SDS, 0.2% bromophenol blue, 40% glycerol, and 20% β -mercaptoethanol), boiled at 90 °C for 10 min, and the supernatant directly loaded on SDS-PAGE using the Bio-Rad Mini-PROTEAN system (Bio-Rad).

Polysome profiling

Eight-day-old seedlings expressing *proeIF3M1-eIF3M1::mCherry* and *peIF3M2-eIF3M2::mCherry* constructs were collected from control conditions and after HS treatment. All the seedlings were planted at the same time and divided into 3 parts as biological replicates, and plants were quickly frozen in liquid nitrogen, ground to powder, and resuspended in 1:3 ratio of polysome extraction buffer (200 mM Tris-HCl pH 9.0, 200 mM KCl, 36 mM MgCl₂, 25 mM EGTA, 1% Triton X-100, 1% Tween 20, 2% polyoxyethylene cholate, 5 mM DTT, 25 μ g/mL cycloheximide, 1% Brij-35, and 2% deoxycholic acid). The solution was loaded on top of 10% to 45% sucrose density gradient in Beckmann 13.5-mL ultracentrifuge tube prepared by Biocomp Gradient Master 108 1 d before and stored overnight at 4 °C. The samples were centrifuged with SW41Ti rotor at $rcf_1 = 110,000 \times g$ for 3 h at 4 °C. The polysome profile was recorded with a chart recorder using a gradient fractionator connected to a UA-5 detector. Three biological replicates were collected. The same procedure was followed for 4 h in vitro PT samples from stable *N. tabacum* transgenic lines expressing *plAt52::AtEIF3M2:YFP* and *plAt52::YFP* 4 h at 28 °C.

BiFC cloning

The Golden Braid 3.0 domesticator software (<https://gbccloning.upv.es/tools/domestication/>) facilitated the in silico domestication of *eIF3M1*, *eIF3M2*, *HSP70-1*, *HSP70-2*, *HSP70-3*, *HSP70-4*, and *eIF4G* genes. Following in silico assembly, domestication oligonucleotides were designed. The Phusion polymerase (Life Technologies) with proofreading activity was used to amplify domesticated fragments intended for cloning into GBparts and subsequent cloning. The purified fragments were cloned in pUPD2 vector backbones. The Cassava promoter (pCsvm) was used for the assembly of all cassettes into complete transcription units. Splitted mVenus for BiFC method was used according to Gookin and Assmann (2014) and Raabe et al. (2024). The constructs were cloned using the GoldenBraid cloning system (Sarrion-Perdigones et al. 2013).

N. benthamiana transient assays

Splitted mVenus BiFC constructs were expressed in pavement cells of *N. benthamiana* to validate the protein interaction between HSP70 and *eIF3M2*. Competent cells of *Agrobacterium tumefaciens* (strain GV3101) were transformed with the appropriate

expression clones and cultured on YEB medium supplemented with gentamicin (50 µg/mL), rifampicin (50 µg/mL), and specific selection agents for each vector (spectinomycin 100 µg/mL) at 28 °C for 48 h. Afterward, colonies were inoculated in the same media without agar and grown overnight at 28 °C. The bacterial cells from overnight cultures were then pelleted by centrifugation (5 min at 1,620 × g), washed twice, resuspended, and diluted to an OD₆₀₀ of 0.3 with infiltration medium (10 mM MES pH 5.6, 10 mM MgCl₂, and 200 µM acetosyringone). A suspension containing cells carrying the p19 repressor plasmid (with kanamycin selection, 50 µg/mL) was added at a 1:1 ratio with other suspensions to prevent gene silencing and enhance transient expression. The mixed suspensions were incubated with moderate shaking for 3 h at room temperature and then injected into the abaxial side of 4-wk-old *N. benthamiana* leaves. Forty-eight to seventy-two hours after infiltration, *N. benthamiana* epidermal cells were examined microscopically.

Accession numbers

Sequence data from this article can be found in the GenBank/EMBL data libraries under accession numbers listed in [Supplementary Table S2](#).

Acknowledgments

We kindly acknowledge Oldřich Navrátil (IEB) for help with generating *N. tabacum* stable lines. We also acknowledge the Imaging Facility of the Institute of Experimental Botany AS CR supported by the MEYS CR (LM2023050 Czech-BioImaging) and IEB AS CR.

Author contributions

S.H., C.M., and Z.K. designed the study. Z.K. performed the experiments with help from C.M., K.R., S.H., and V.K. Z.K. and S.H. wrote the manuscript. S.H., Z.K., C.M., K.R., V.K., and D.H. edited the manuscript. All authors approved the final manuscript.

Supplementary data

The following materials are available in the online version of this article.

Supplementary Figure S1. Phenotypic analysis of *eif3m1* and *eif3m2* mutants.

Supplementary Figure S2. In vivo pollen germination is not affected in *eif3m1*, *eif3m2*, or double mutant.

Supplementary Figure S3. Validations of eIF3M2 and HSP70 upregulated promoter HSR.

Supplementary Figure S4. eIF3M1 is expressed in mature pollen grains and eIF3M2 detected in the early stages of male gametophyte.

Supplementary Table S1. List of primers.

Supplementary Table S2. Accession numbers.

Funding

This study received financial support from the European Regional Development Fund (ERDF) Programme Johannes Amos Comenius project TowArds Next GENERation Crops (TANGENC) (reg. no. CZ.02.01.01/00/22_008/0004581) and by the Czech Science Foundation GACR grant nos. 22-29717S and 24-10653S.

Conflict of interest statement. None declared.

Data availability

The data underlying this article are available in the article and in its online supplementary material.

References

- Berka M, Kopecká R, Berková V, Brzobohatý B, Černý M. Regulation of heat shock proteins 70 and their role in plant immunity. *J Exp Bot*. 2022;73(7):1894–1909. <https://doi.org/10.1093/jxb/erab549>
- Billey E, Hafidh S, Cruz-Gallardo I, Litholdo CGJR, Jean V, Carpentier MC, Bousquet-Antonelli C. LARP6C orchestrates posttranscriptional reprogramming of gene expression during hydration to promote pollen tube guidance. *Plant Cell*. 2021;33(8):2637–2661. <https://doi.org/10.1093/plcell/koab131>
- Blazie SM, Takayanagi-Kiya S, McCulloch KA, Jin Y. Eukaryotic initiation factor EIF-3.G augments mRNA translation efficiency to regulate neuronal activity. *ELife*. 2021;10:e68336. <https://doi.org/10.7554/eLife.68336>
- Boavida LC, McCormick S. Temperature as a determinant factor for increased and reproducible in vitro pollen germination in *Arabidopsis thaliana*. *Plant J*. 2007;52(3):570–582. <https://doi.org/10.1111/j.1365-313X.2007.03248.x>
- Browning KS, Bailey-Serres J. Mechanism of cytoplasmic mRNA translation. *Arabidopsis Book*. 2015;13:e0176. <https://doi.org/10.1199/tab.0176>
- Cattie DJ, Richardson CE, Reddy KC, Ness-Cohn EM, Droste R, Thompson MK, Gilbert WV, Kim DH. Mutations in nonessential eIF3k and eIF3l genes confer lifespan extension and enhanced resistance to ER stress in *Caenorhabditis elegans*. *PLoS Genet*. 2016;12(9):e1006326. <https://doi.org/10.1371/journal.pgen.1006326>
- Chaturvedi P, Wiese AJ, Ghatak A, Závěská Drábková L, Weckwerth W, Honys D. Heat shock response mechanisms in pollen development. *New Phytol*. 2021;231(2):571–585. <https://doi.org/10.1111/nph.17380>
- Clough SJ, Bent AF. Floral dip: a simplified method for *Agrobacterium*-mediated transformation of *Arabidopsis thaliana*. *Plant J*. 1998;16(6):735–743. <https://doi.org/10.1046/j.1365-313x.1998.00343.x>
- Dai P, Wang X, Gou L-T, Li Z-T, Wen Z, Chen Z-G, Hua M-M, Zhong A, Wang L, Su H, et al. A translation-activating function of MIWI/piRNA during mouse spermiogenesis. *Cell*. 2019;179(7):1566–1581.e16. <https://doi.org/10.1016/j.cell.2019.11.022>
- Dai X, Zhu M. Coupling of ribosome synthesis and translational capacity with cell growth. *Trends Biochem Sci*. 2020;45(8):681–692. <https://doi.org/10.1016/j.tibs.2020.04.010>
- Desroches Altamirano C, Kang M-K, Jordan MA, Borianne T, Dilmen I, Gnädig M, von Appen A, Honigsmann A, Franzmann TM, Alberti S. eIF4F is a thermo-sensing regulatory node in the translational heat shock response. *Mol Cell*. 2024;84(9):1727–1741.e12. <https://doi.org/10.1016/j.molcel.2024.02.038>
- Duan H, Zhang S, Zarai Y, Öllinger R, Wu Y, Sun L, Hu C, He Y, Tian G, Rad R, et al. eIF3 mRNA selectivity profiling reveals eIF3k as a cancer-relevant regulator of ribosome content. *EMBO J*. 2023;42(12):e112362. <https://doi.org/10.15252/embj.2022112362>
- Dutt S, Parkash J, Mehra R, Sharma N, Singh B, Raigond P, Joshi A, Chopra S, Singh BP. Translation initiation in plants: roles and implications beyond protein synthesis. *Biologia Plantarum*. 2015;59(3):401–412. <https://doi.org/10.1007/s10535-015-0517-y>
- Fragkostefanakis S, Mesihovic A, Hu Y, Schleiff E. Unfolded protein response in pollen development and heat shock tolerance. *Plant Reprod*. 2016;29(1-2):81–91. <https://doi.org/10.1007/s00497-016-0276-8>
- Fujii K, Zhulyn O, Byeon GW, Genuth NR, Kerr CH, Walsh EM, Barna M. Controlling tissue patterning by translational regulation of

- signaling transcripts through the core translation factor eIF3c. *Dev Cell*. 2021;56(21):2928–2937.e9. <https://doi.org/10.1016/j.devcel.2021.10.009>
- Garde R, Dea A, Herwig MF, Pincus D. Feedback control of the heat shock response by spatiotemporal regulation of Hsp70. *J Cell Biol*. 2024;223(12):e202401082. <https://doi.org/10.1083/jcb.202401082>
- Gookin TE, Assmann SM. Significant reduction of Bi FC non-specific assembly facilitates in planta assessment of heterotrimeric G-protein interactors. *Plant J*. 2014;80(3):553–567. <https://doi.org/10.1111/tpj.12639>
- Hafidh S, Fila J, Honys D. Male gametophyte development and function in angiosperms: a general concept. *Plant Reprod*. 2016;29(1-2):31–51. <https://doi.org/10.1007/s00497-015-0272-4>
- Hafidh S, Honys D. Reproduction multitasking: the male gametophyte. *Annu Rev Plant Biol*. 2021;72(1):581–614. <https://doi.org/10.1146/annurev-arplant-080620-021907>
- Hafidh S, Potěšil D, Müller K, Fila J, Michailidis C, Herrmannová A, Feciková J, Ischebeck T, Valášek LS, Zdráhal Z, et al. Dynamics of the pollen sequestrome defined by subcellular coupled omics. *Plant Physiol*. 2018;178(1):258–282. <https://doi.org/10.1104/pp.18.00648>
- Hater F, Nakel T, Gro-Hardt R. Reproductive multitasking: the female gametophyte. *Annu Rev Plant Biol*. 2020;71(1):517–546. <https://doi.org/10.1146/annurev-arplant-081519-035943>
- Hedhly A, Hormaza JI, Herrero M. Global warming and sexual plant reproduction. *Trends Plant Sci*. 2009;14(1):30–36. <https://doi.org/10.1016/j.tplants.2008.11.001>
- Honys D, Reňák D, Feciková J, Jedelský PL, Nebesářová J, Dobrev P, Čapková V. Cytoskeleton-associated large RNP complexes in tobacco male gametophyte (EPPs) are associated with ribosomes and are involved in protein synthesis, processing, and localization. *J Proteome Res*. 2009;8(4):2015–2031. <https://doi.org/10.1021/pr8009897>
- Hong S-W, Vierling E. Mutants of *Arabidopsis thaliana* defective in the acquisition of tolerance to high temperature stress. *Proc Natl Acad Sci U S A*. 2000;97(8):4392–4397. <https://doi.org/10.1073/pnas.97.8.4392>
- Horsch RB, Fry JE, Hoffmann NL, Eichholtz D, Rogers SG, Fraley RT. A simple and general method for transferring genes into plants. *Science*. 1985;227(4691):1229–1230. <https://doi.org/10.1126/SCIENCE.227.4691.1229>
- Jiang Y, Bueckert R, Warkentin T, Davis AR. High temperature effects on in vitro pollen germination and seed set in field pea. *Can J Plant Sci*. 2017;98:71–80. <https://doi.org/10.1139/CJPS-2017-0073>
- Johnson MA, Harper JF, Palanivelu R. A fruitful journey: pollen tube navigation from germination to fertilization. *Annu Rev Plant Biol*. 2019;70(1):809–837. <https://doi.org/10.1146/annurev-arplant-050718-100133>
- Kotak S, Larkindale J, Lee U, von Koskull-Döring P, Vierling E, Scharf K-D. Complexity of the heat shock response in plants. *Curr Opin Plant Biol*. 2007;10(3):310–316. <https://doi.org/10.1016/j.pbi.2007.04.011>
- Kmieciak SW, Le Breton L, Mayer MP. Feedback regulation of heat shock factor 1 (Hsf1) activity by Hsp70-mediated trimer unzipping and dissociation from DNA. *EMBO J*. 2020;39(14):e104096. <https://doi.org/10.15252/embj.2019104096>
- Kumar V, Hafidh S. A protocol for in vivo RNA labeling and visualization in tobacco pollen tubes. *STAR Protoc*. 2024;5(4):103433. <https://doi.org/10.1016/j.xpro.2024.103433>
- Lalanne E, Twell D. Genetic control of male germ unit organization in *Arabidopsis*. *Plant Physiol*. 2002;129(2):865–875. <https://doi.org/10.1104/pp.003301>
- Lin Y, Li F, Huang L, Polte C, Duan H, Fang J, Sun L, Xing X, Tian G, Cheng Y, et al. eIF3 associates with 80S ribosomes to promote translation elongation, mitochondrial homeostasis, and muscle health. *Mol Cell*. 2020;79(4):575–587.e7. <https://doi.org/10.1016/j.molcel.2020.06.003>
- Lin B-L, Wang J-S, Liu H-C, Chen R-W, Meyer Y, Barakat A, Delseny M. Genomic analysis of the Hsp70 superfamily in *Arabidopsis thaliana*. *Cell Stress Chaperones*. 2001;6(3):201–208. [https://doi.org/10.1379/1466-1268\(2001\)006<0201:GAOTHS>2.0.CO;2](https://doi.org/10.1379/1466-1268(2001)006<0201:GAOTHS>2.0.CO;2)
- Li Q, Deng Z, Gong C, Wang T. The rice eukaryotic translation initiation factor 3 subunit f (OseIF3f) is involved in microgametogenesis. *Front Plant Sci*. 2016;7:2016. <https://doi.org/10.3389/fpls.2016.00532>
- Llácer JL, Hussain T, Dong J, Villamayor L, Gordiyenko Y, Hinnebusch AG. Large-scale movement of eIF3 domains during translation initiation modulate start codon selection. *Nucleic Acids Res*. 2021;49(20):11491–11511. <https://doi.org/10.1093/nar/gkab908>
- Matsuoka E, Kato N, Hara M. Induction of the heat shock response in *Arabidopsis* by heat shock protein 70 inhibitor VER-155008. *Funct Plant Biol*. 2019;46(10):925. <https://doi.org/10.1071/FP18259>
- Mori T, Kuroiwa H, Higashiyama T, Kuroiwa T. GENERATIVE CELL SPECIFIC 1 is essential for angiosperm fertilization. *Nat Cell Biol*. 2006;8(1):64–71. <https://doi.org/10.1038/ncb1345>
- Murashige T, Skoog F. A revised medium for rapid growth and bioassays with tobacco tissue cultures. *Physiol Plant*. 1962;15(3):473–497. <https://doi.org/10.1111/j.1399-3054.1962.tb08052.x>
- Noack LC, Pejchar P, Sekereš J, Jaillais Y, Potocký M. Transient gene expression as a tool to monitor and manipulate the levels of acidic phospholipids in plant cells. *Methods Mol Biol*. 2019;1992:189–199. https://doi.org/10.1007/978-1-4939-9469-4_12
- Ohama N, Kusakabe K, Mizoi J, Zhao H, Kidokoro S, Koizumi S, Takahashi F, Ishida T, Yanagisawa S, Shinozaki K, et al. The transcriptional cascade in the heat shock response of *Arabidopsis* is strictly regulated at the level of transcription factor expression. *Plant Cell*. 2016;28(1):181–201. <https://doi.org/10.1105/tpc.15.00435>
- Park C-J, Seo Y-S. Heat shock proteins: a review of the molecular chaperones for plant immunity. *Plant Pathol J*. 2015;31(4):323–333. <https://doi.org/10.5423/PPJ.RW.08.2015.0150>
- Parrotta L, Cresti M, Cai G. Heat-shock protein 70 binds microtubules and interacts with kinesin in tobacco pollen tubes. *Cytoskeleton*. 2013;70(9):522–537. <https://doi.org/10.1002/cm.21134>
- Parrotta L, Faleri C, Guerriero G, Cai G. Cold stress affects cell wall deposition and growth pattern in tobacco pollen tubes. *Plant Sci*. 2019;283:329–342. <https://doi.org/10.1016/j.plantsci.2019.03.010>
- Poidevin L, Forment J, Unal D, Ferrando A. Transcriptome and translational changes in germinated pollen under heat shock uncover roles of transporter genes involved in pollen tube growth. *Plant Cell Environ*. 2021;44(7):2167–2184. <https://doi.org/10.1111/pce.13972>
- Raabe K, Honys D, Michailidis C. The role of eukaryotic initiation factor 3 in plant translation regulation. *Plant Physiol Biochem*. 2019;145:75–83. <https://doi.org/10.1016/j.plaphy.2019.10.015>
- Raabe K, Náprstková A, Pieters J, Torutaeva E, Jirásková V, Kahrizi Z, Michailidis C, Honys D. Implementation of Ribo-BiFC method to plant systems using a split mVenus approach. *bioRxiv* 2024.09.12.612679. <https://doi.org/10.1101/2024.09.12.612679>, 17 September 2024, preprint: not peer reviewed.
- Rausell A, Kanhonou R, Yenush L, Serrano R, Ros R. The translation initiation factor eIF1A is an important determinant in the tolerance to NaCl stress in yeast and plants. *Plant J*. 2003;34(3):257–267. <https://doi.org/10.1046/j.1365-313X.2003.01719.x>
- Ren R, Jiang X, Di W, Li Z, Li B, Xu J, Liu Y. HSP70 improves the viability of cryopreserved *Paeonia lactiflora* pollen by regulating oxidative stress and apoptosis-like programmed cell death events. *Plant Cell Tissue Organ Cult*. 2019;139(1):53–64. <https://doi.org/10.1007/s11240-019-01661-z>

- Rodriguez-Enriquez MJ, Mehdi S, Dickinson HG, Grant-Downton RT. A novel method for efficient in vitro germination and tube growth of *Arabidopsis thaliana* pollen. *New Phytol.* 2013;197(2):668–679. <https://doi.org/10.1111/nph.12037>
- Rosenzweig R, Nillegoda NB, Mayer MP, Bukau B. The Hsp70 chaperone network. *Nat Rev Mol Cell Biol.* 2019;20(11):665–680. <https://doi.org/10.1038/s41580-019-0133-3>
- Roy B, Copenhaver GP, von Arnim AG. Fluorescence-tagged transgenic lines reveal genetic defects in pollen growth-application to the eIF3 complex. *PLoS One.* 2011;6(3):e17640. <https://doi.org/10.1371/journal.pone.0017640>
- Sable A, Rai KM, Choudhary A, Yadav VK, Agarwal SK, Sawant SV. Inhibition of Heat Shock proteins HSP90 and HSP70 induce oxidative stress, suppressing cotton fiber development. *Sci Rep.* 2018;8(1):3620. <https://doi.org/10.1038/s41598-018-21866-0>
- Sarrion-Perdigones A, Vazquez-Vilar M, Palací J, Castelijn B, Forment J, Ziarsolo P, Blanca J, Granell A, Orzaez D. GoldenBraid 2.0: a comprehensive DNA assembly framework for plant synthetic biology. *Plant Physiol.* 2013;162(3):1618–1631. <https://doi.org/10.1104/PP.113.217661>
- Shah M, Su D, Scheliga JS, Pluskal T, Boronat S, Motamedchaboki K, Campos AR, Qi F, Hidalgo E, Yanagida M, et al. A transcript-specific eIF3 complex mediates global translational control of energy metabolism. *Cell Rep.* 2016;16(7):1891–1902. <https://doi.org/10.1016/j.celrep.2016.07.006>
- Son S, Park SR. Plant translational reprogramming for stress resilience. *Front Plant Sci.* 2023;14:1151587. <https://doi.org/10.3389/fpls.2023.1151587>
- Sze H, Palanivelu R, Harper JF, Johnson MA. Holistic insights from pollen omics: co-opting stress-responsive genes and ER-mediated proteostasis for male fertility. *Plant Physiol.* 2021;187(4):2361–2380. <https://doi.org/10.1093/plphys/kiab463>
- Tahmasebi S, Sonenberg N, Hershey JWB, Mathews MB. Protein synthesis and translational control: a historical perspective. *Cold Spring Harb Perspect Biol.* 2019;11(9):a035584. <https://doi.org/10.1101/cshperspect.a035584>
- Tiwari LD, Kumar R, Sharma V, Sahu AK, Sahu B, Naithani SC, Grover A. Stress and development phenotyping of Hsp101 and diverse other Hsp mutants of *Arabidopsis thaliana*. *J Plant Biochem Biotechnol.* 2021;30(4):889–905. <https://doi.org/10.1007/S13562-021-00706-9>
- Ul Haq S, Khan A, Ali M, Khattak AM, Gai W-X, Zhang HX, Wei AM, Gong ZH. Heat shock proteins: dynamic biomolecules to counter plant biotic and abiotic stresses. *Int J Mol Sci.* 2019;20(21):5321. <https://doi.org/10.3390/ijms20215321>
- Urquidí Camacho RA, Lokdarshi A, von Arnim AG. Translational gene regulation in plants: a green new deal. *Wiley Interdiscip Rev RNA.* 2020;11(6):e1597. <https://doi.org/10.1002/wrna.1597>
- Usman MG, Rafii MY, Martini MY, Yusuff OA, Ismail MR, Miah G. Molecular analysis of Hsp70 mechanisms in plants and their function in response to stress. *Biotechnol Genet Eng Rev.* 2017;33(1):26–39. <https://doi.org/10.1080/02648725.2017.1340546>
- Valášek LS, Zeman J, Wagner S, Beznosková P, Pavlíková Z, Mohammad MP, Hronová V, Herrmannová A, Hashem Y, Gunišová S. Embraced by eIF3: structural and functional insights into the roles of eIF3 across the translation cycle. *Nucleic Acids Res.* 2017;45(19):10948–10968. <https://doi.org/10.1093/nar/gkx805>
- Vergne P, Delvallee I, Dumas C. Rapid assessment of microspore and pollen development stage in wheat and maize using DAPI and membrane permeabilization. *Stain Technol.* 1987;62(5):299–304. <https://doi.org/10.3109/10520298709108014>
- Wang M, Wei K, Qian B, Feiler S, Lemekhova A, Büchler MW, Hoffmann K. HSP70–eIF4G interaction promotes protein synthesis and cell proliferation in hepatocellular carcinoma. *Cancers (Basel).* 2020;12(8):2262. <https://doi.org/10.3390/cancers12082262>
- Wagner S, Herrmannová A, Šikrová D, Valášek LS. Human eIF3b and eIF3a serve as the nucleation core for the assembly of eIF3 into two interconnected modules: the yeast-like core and the octamer. *Nucleic Acids Res.* 2016;44(22):10772–10788. <https://doi.org/10.1093/nar/gkw972>
- Wolf DA, Lin Y, Duan H, Cheng Y. EIF-Three to Tango: emerging functions of translation initiation factor eIF3 in protein synthesis and disease. *J Mol Cell Biol.* 2020;12(6):403–409. <https://doi.org/10.1093/jmcb/mjaa018>
- Xu J, Zhang B, Jiang C, Ming F. RceIF5A, encoding a eukaryotic translation initiation factor 5A in *Rosa chinensis*, can enhance thermotolerance, oxidative and osmotic stress resistance of *Arabidopsis thaliana*. *Plant Mol Biol.* 2011;75(1-2):167–178. <https://doi.org/10.1007/s11103-010-9716-2>
- Zeng L, Wan Y, Li D, Wu J, Shao M, Chen J, Hui L, Ji H, Zhu X. The m subunit of murine translation initiation factor eIF3 maintains the integrity of the eIF3 complex and is required for embryonic development, homeostasis, and organ size control. *J Biol Chem.* 2013;288(42):30087–30093. <https://doi.org/10.1074/jbc.M113.506147>
- Zhang L, Liu X, Gaikwad K, Kou X, Wang F, Tian X, Xin M, Ni Z, Sun Q, Peng H, et al. Mutations in eIF5B confer thermosensitive and pleiotropic phenotypes via translation defects in *Arabidopsis thaliana*. *Plant Cell.* 2017;29(8):1952–1969. <https://doi.org/10.2307/90012853>